Physics – Uspekhi **66** (8) 753 – 774 (2023)

REVIEWS OF TOPICAL PROBLEMS PACS numbers: 14.60.Lm, 14.60.Pq

Neutrino oscillations: status and prospects for the determination of neutrino mass ordering and the leptonic *CP*-violation phase

L D Kolupaeva, M O Gonchar, A G Olshevskiy, O B Samoylov

DOI: https://doi.org/10.3367/UFNe.2022.05.039191

Contents

Abstract. This review is devoted to the 110th anniversary of the birth of Bruno Pontecorvo, an outstanding physicist who made an invaluable contribution to the development of modern neutrino physics, having predicted, inter alia, nonzero neutrino masses, mixing, and oscillations that were experimentally discovered in the early 2000s. Significant progress has been made over 20 years of experiments in determining the parameters of three-flavor neutrino oscillations. The status of and prospects for establishing neutrino mass ordering and the leptonic *CP*-violation phase (δ_{CP}), unknown parameters of this theory, are discussed. It is expected that they will be measured in long-baseline experiments in the next decade. The ongoing accelerator experiments NOvA and T2K, which are currently the most sensitive to neutrino mass ordering and δ_{CP}, are described in detail. For ease of comparison, NOvA and T2K techniques and results, including all aspects of data collection and analysis, are presented on a stage-by-stage basis. Possible reasons for the disagreement between the δ_{CP} values measured by NOvA and T2K are discussed. Future accelerator (DUNE and Hyper-Kamiokande) and reactor (JUNO) megaprojects are considered, along with experiments designed to use atmospheric neutrinos: IceCube Upgrade, KM3NeT (ORCA), and ICAL at INO, which can measure unknown oscillation parameters and refine the ones already determined.

Keywords: neutrinos, neutrino oscillations, mass hierarchy, leptonic *CP* violation, accelerator neutrinos, reactor neutrinos, atmospheric neutrinos, solar neutrinos

L D Kolupaeva [(a)], **M O Gonchar** [(b)], **A G Olshevskiy** [(c)], **O B Samoylov** [(d)]
Joint Institute for Nuclear Research,
ul. Joliot-Curie 6, 141980 Dubna, Moscow region, Russian Federation
E-mail: [(a)] ldkolupaeva@yandex.ru, [(b)] gonchar@jinr.ru,
[(c)] olshevsk@jinr.ru, [(d)] samoylov@jinr.ru

Received 17 January 2022, revised 5 May 2022
Uspekhi Fizicheskikh Nauk **193** (8) 801 – 824 (2023)
Translated by M Zh Shmatikov

Dedicated to the 110th anniversary of the birth of Bruno Pontecorvo, a founder of modern neutrino physics, who predicted neutrino oscillations

1. Introduction

In 2022, the neutrino oscillation hypothesis, first put forward in 1957 by the Italian and Soviet physicist Bruno Maksimovich Pontecorvo, turned 65 years old [1–4]. This model, which was further developed in many of his works, including joint studies with V N Gribov [5] and S M Bilenkii [6, 7], and studies by Z Maki, M Nakagawa, and S Sakata, who proposed the idea of flavor mixing [8], by the end of the 1970s already contained the main components of the theory of neutrino oscillations.

The idea of neutrino oscillations anticipated even indirect experimental indications of their existence — a deficit of solar neutrinos and an anomaly in the atmospheric neutrino [9–14]. More than 40 years of experimental research were needed to fully confirm neutrino oscillations: at the turn of the 20th and 21st centuries, neutrino oscillations were discovered by the Super-Kamiokande [15] and SNO [1] [17] experiments, which were awarded the 2015 Nobel Prize.

Since the beginning of the 21st century. the physics of neutrino oscillations has focused on the precise measurement of the parameters that determine the process it studies. The prestigious 2016 Breakthrough Prize [18] was awarded to five experiments — Super-Kamiokande, SNO, KamLAND (Kamioka Liquid scintillator Anti-Neutrino Detector) [19], T2K/K2K (Tokai to Kamioka/KEK to Kamioka) [20, 21], and Daya Bay [22] — for, as formulated in the text of the award, the detection and study of neutrino oscillations, which opened up new frontiers beyond the Standard Model (SM) of particle physics.

Neutrino oscillations, as an indication of small but nonzero masses of these particles due to the unknown mechanism of their origin, despite the technical possibility

[1] It should be noted that actually the Sudbury Neutrino Observatory (SNO) discovered the phenomenon of adiabatic flavor transitions [16] of neutrinos in matter on the Sun.

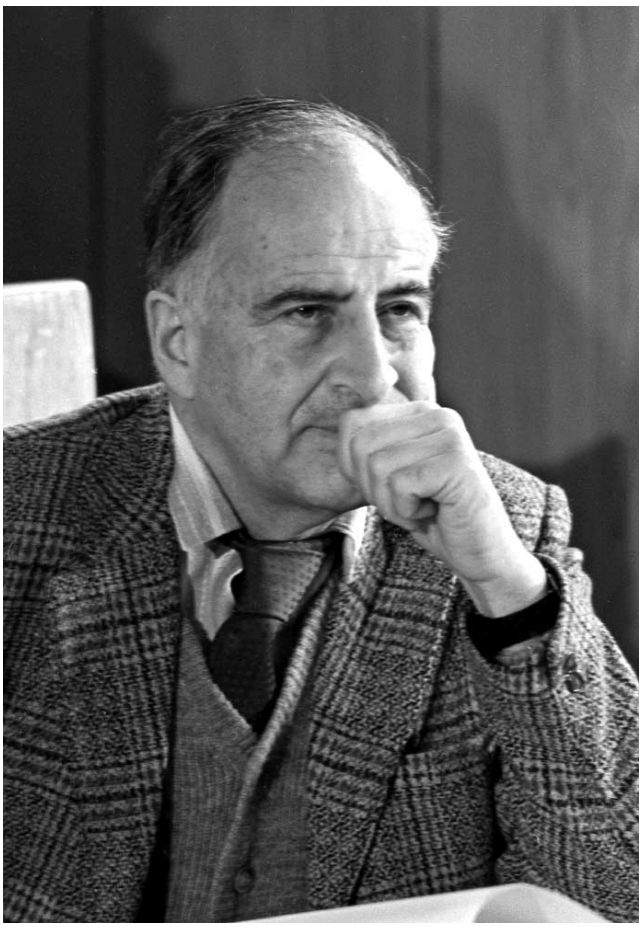

Bruno Maksimovich Pontecorvo
(22.08.1913 – 24.09.1993)

of their generation by introducing right-handed components, are often interpreted as evidence of physics beyond the SM [23–27].

In addition to studying oscillations in neutrino physics, searches are underway for hypothetical sterile neutrinos [28, 29], the discovery of which would be a direct indication of phenomena beyond the SM, similar to the discovery of a signal from neutrinoless double beta decay [30–32], indicating the Majorana nature of neutrinos.

Active attempts are being made to directly measure the neutrino mass. At the time of writing this review, the strongest limitation was obtained in the KATRIN (KArlsruhe TRItium Neutrino) experiment [33] with 1/50 of the planned statistics: $m_\nu < 0.8$ eV with a confidence level (CL) of 90%.

The study of neutrino fluxes from various sources is also a vibrant topic of research. Astrophysical [34–36] neutrinos and the search for sources of ultrahigh-energy neutrinos deserve special mention. A notable recent discovery was also the detection of neutrinos from the CNO cycle in the Sun in the Borexino experiment [37, 38].

This review, the scope of which does not include the most interesting issues listed above, is focused on the oscillations of three types of neutrinos, namely, current and future experiments with a long baseline sensitive to still unmeasured parameters: the neutrino mass hierarchy and the phase of *CP* violation in the lepton sector.

Neutrino oscillations are periodic transitions between the flavors of these particles propagating in matter or vacuum [39–41]. Neutrino oscillations are possible due to their nonzero masses, which are not equal, and to the presence of mixing.

Flavor neutrinos ν_e, ν_μ, ν_τ are a linear combination of mass neutrinos ν_1, ν_2, ν_3: $\nu_{\alpha,L} = \sum_{i=1,2,3} U_{\alpha i}\,\nu_{i,L}$. Mixing matrix U in a vacuum, which is called the Pontecorvo–Maki–Nakagawa–Sakata (PMNS) matrix, can be parameterized as follows:

$$U = \begin{pmatrix} 1 & 0 & 0 \\ 0 & c_{23} & s_{23} \\ 0 & -s_{23} & c_{23} \end{pmatrix} \times \begin{pmatrix} c_{13} & 0 & s_{13}\exp(-\mathrm{i}\delta_{CP}) \\ 0 & 1 & 0 \\ -s_{13}\exp(\mathrm{i}\delta_{CP}) & 0 & c_{13} \end{pmatrix} \times \begin{pmatrix} c_{12} & s_{12} & 0 \\ -s_{12} & c_{12} & 0 \\ 0 & 0 & 1 \end{pmatrix}, \quad (1)$$

where $c_{ij} = \cos\theta_{ij}$ and $s_{ij} = \sin\theta_{ij}$. Formula (1) contains the mixing angles θ_{12}, θ_{23}, θ_{13} and the phase of *CP* violation in the lepton sector, δ_{CP}.

Possible Majorana phases are omitted in Eqn (1), since oscillation experiments are not sensitive to them. The PMNS matrix is similar to the Cabibbo–Kobayashi–Maskawa (CKM) matrix in the quark sector, but the mixing in the lepton matrix differs significantly from that in the nearly diagonal CKM matrix.

The probabilities of oscillations of three types of neutrinos in a vacuum in the general case, under the condition of unitarity of the mixing matrix, are determined by the following formula:

$$P(\nu_\alpha \to \nu_\beta) = \delta_{\alpha\beta} - 4\sum_{i<j} \mathrm{Re}\left[U_{\alpha i}U^*_{\beta i}U^*_{\alpha j}U_{\beta j}\right]\sin^2\frac{\Delta m^2_{ij}L}{4E} + 2\sum_{i<j}\mathrm{Im}\left[U_{\alpha i}U^*_{\beta i}U^*_{\alpha j}U_{\beta j}\right]\sin\frac{\Delta m^2_{ij}L}{2E}. \quad (2)$$

As can be seen from Eqn (2), the probabilities of neutrino oscillations depend not only on the elements of the mixing matrix $U_{\alpha i}$ but also on the differences among the squares of the neutrino masses $\Delta m^2_{ij} = m^2_i - m^2_j$, $i \neq j = 1, 2, 3$, and on the distance L between the detector and the source and energy E. A model with wave packets [42, 43] introduces corrections to formula (2) related to the representation of mass neutrinos in the form of wave packets moving at different velocities. When the packets diverge, coherence is lost, thereby leading to the suppression of oscillations (decoherence). Currently, the Daya Bay experiment alone provides restrictions on the relative dispersion of momentum [44]: $\sigma_{\mathrm{rel}} < 0.23$, which corresponds to the restriction on the width of the wave packet from below $\sigma_x > 10^{-11}$ cm. Oscillations are suppressed if the condition $L \gtrsim L^{\mathrm{coherence}}_{kj} = 4\sqrt{2}E^2\sigma_x/\Delta m^2_{kj}$ is satisfied. In this review, we do not consider decoherence effects.

When a neutrino propagates in a dense medium, an additional potential arises in the Hamiltonian for electron neutrinos [45], which can interact with electrons of matter not only through neutral but also through charged currents. The oscillation probabilities are described then by the effective mixing angles and neutrino masses. This feature is clearly manifested in considering neutrino fluxes from the Sun. When the density of matter varies, the oscillation amplitude can reach the maximum possible value, even if mixing in a

vacuum is small. This phenomenon was named the MSW resonance in honor of S P Mikheev, A Yu Smirnov [46, 47], and L Wolfenstein [45], who predicted this effect.

In the case of oscillations of three types of neutrinos in matter with a constant density, explicit formulas for $P(\nu_\alpha \to \nu_\beta)$ can be expressed in terms of oscillation parameters as [49]

$$P(\nu_\mu \to \nu_e) \approx \sin^2\theta_{23}\sin^2(2\theta_{13})\,\frac{\sin^2\left[\Delta(1-A)\right]}{(1-A)^2} + \alpha\widetilde{J}\cos(\Delta \pm \delta_{CP})\,\frac{\sin(\Delta A)}{A}\,\frac{\sin\left[\Delta(1-A)\right]}{1-A} + \alpha^2\cos^2\theta_{23}\sin^2(2\theta_{12})\,\frac{\sin^2(\Delta A)}{A^2}, \quad (3)$$

where $\Delta = \Delta m^2_{31}L/(4E)$, $A = \pm 2\sqrt{2}G_F n_e E/\Delta m^2_{32}$, G_F is the Fermi constant, $\widetilde{J} = \cos\theta_{13}\sin(2\theta_{13})\sin(2\theta_{12})\sin(2\theta_{23})$, and the sign before δ_{CP} on the right side of the formula, as in the definition of A, is different for neutrinos (+) and antineutrinos (−). The formula for the oscillation probabilities was obtained by diagonalizing the Hamiltonian with terms retained up to the second order of smallness in $\alpha = \Delta m^2_{21}/\Delta m^2_{31}$ [50].

If the final detectable neutrino flavor coincides with the initial one, the probability of neutrino survival/disappearance is introduced. The formula for the survival probability of electron antineutrinos in a vacuum, which is also used in reactor experiments, is

$$P(\bar{\nu}_e \to \bar{\nu}_e) = 1 - \sin^2(2\theta_{12})\cos^4\theta_{13}\sin^2\frac{\Delta m^2_{21}L}{4E} - \sin^2(2\theta_{13})\left(\sin^2\theta_{12}\sin^2\frac{\Delta m^2_{32}L}{4E} + \cos^2\theta_{12}\sin^2\frac{\Delta m^2_{31}L}{4E}\right). \quad (4)$$

Depending on the base length, reactor experiments can be sensitive to four parameters of neutrino oscillations: $|\Delta m^2_{32}|$ ($|\Delta m^2_{31}|$), Δm^2_{21}, $\sin^2(2\theta_{13})$, and $\sin^2(2\theta_{12})$; in this case, there is no dependence on the phase of violation of CP invariance and $\sin^2\theta_{23}$.

For the energy range of reactor antineutrinos, depending on the distances, the following types of experiments are distinguished: with a small base (5–30 m), which are sensitive to sterile neutrinos with squared mass differences in the range[2] $10^{-2} \lesssim \Delta m^2_{41} \lesssim 10$ eV^2 and $\sin^2(2\theta_{14})$; with a medium base (1–2 km, Daya Bay, RENO (Reactor Experiment for Neutrino Oscillation), Double Chooz), which are sensitive to $|\Delta m^2_{32}|$ and $\sin^2(2\theta_{13})$; and with a long base (> 10 km, KamLAND, JUNO (Jiangmen Underground Neutrino Observatory)), which are sensitive to $|\Delta m^2_{32}|$, Δm^2_{21}, $\sin^2(2\theta_{12})$ and, to a lesser extent, to $\sin^2(2\theta_{13})$.

At a base of around 53 km (JUNO), sensitivity to the neutrino mass hierarchy appears. The effect of neutrino interaction with matter at small and medium bases is negligible, while at large bases it contributes up to 4% [51, 52].

By measuring the transition probabilities of various types of neutrinos in matter or vacuum, conclusions are drawn about the oscillation parameters, which are basic characteristics of the SM lepton sector.

[2] Oscillation parameters are quoted for the case where a fourth hypothetical neutrino exists. The theory and status of the search for a light sterile neutrino are presented in more detail in review [28].

2. Current status of measurement of oscillation parameters

2.1 Mixing angles and squared mass differences

Since the beginning of the 21st century, some parameters have been precisely measured in a number of experiments [53]. To date, most of these parameters have been measured with an accuracy of a few percent [54]. The fundamental task of neutrino physics is to construct a theory that would explain, first of all, the smallness of neutrino masses and large mixing. Various available models can be checked by comparing their predictions with experimental measurements. In particular, the models of neutrino mass generation and flavor symmetries [55] predict various relationships [56] for the mixing parameters, so-called sum rules. The possibility of using these relations as a hypothesis test is limited by the accuracy with which the oscillation parameters are measured. Neutrino masses can also be included in such expressions, which can make it possible to establish theoretical restrictions on the absolute values of the masses in the models under consideration. According to some Grand Unification theories, the mixing parameters of quarks and leptons should be related [57]. To verify this relationship, the lepton and quark mixing parameters should be known with comparable accuracy. However, at present, the accuracy with which the elements of the lepton mixing matrix are measured is worse than that of the quark matrix: the accuracy of measuring the CKM matrix elements is $\lesssim 6\%$ [23].

2.1.1 Oscillation parameters θ_{12} and Δm^2_{21}. The dominant contribution to the determination of the so-called solar parameters θ_{12} and Δm^2_{21} was made by the SNO, Super-Kamiokande (SK), and KamLAND (Kamioka Liquid scintillator Anti-Neutrino Detector) experiments, which handle solar and reactor neutrino fluxes. The Super-Kamiokande result is always represented in combination with the SNO result. The results of measurements of θ_{12} in all experiments agree well with each other (Fig. 1a).

The survival probability of solar neutrinos is sensitive to oscillation parameters due to the effects of neutrino interaction with matter on the Sun. Additional and fairly strong sensitivity to the value of Δm^2_{21} is also due to the interaction of neutrinos with matter on Earth (asymmetry of registered ν_e-events with solar neutrinos during the day and at night). The first and so far the only experiment that has indicated the existence of asymmetry at the level of several percent for the neutrinos from ^{8}B decay is Super-Kamiokande [62], where the measured asymmetry was $(-3.6 \pm 1.6(\text{stat.}) \pm 0.6(\text{syst.}))\%$.

Super-Kamiokande's preferred value of Δm^2_{21} differed by $\sim 2\sigma$ from KamLAND's result. Since then, the Super-Kamiokande + SNO measurement has consistently preferred a value of Δm^2_{21} lower than that in KamLAND (Fig. 1b). Of importance here is also the relatively large day/night asymmetry that Super-Kamiokande observes for solar neutrinos.

Super-Kamiokande's results [65] presented in 2020 reduced the difference between the Δm^2_{21} measured in reactor and solar experiments, which nevertheless is still 1.4σ. The measured asymmetry is $(-2.1 \pm 1.1)\%$. A possible explanation [66] for the disagreement over the past few years is nonstandard interactions (NSIs) of neutrinos, which are considered in more detail below. However, the decrease in differences between the results reported by KamLAND and

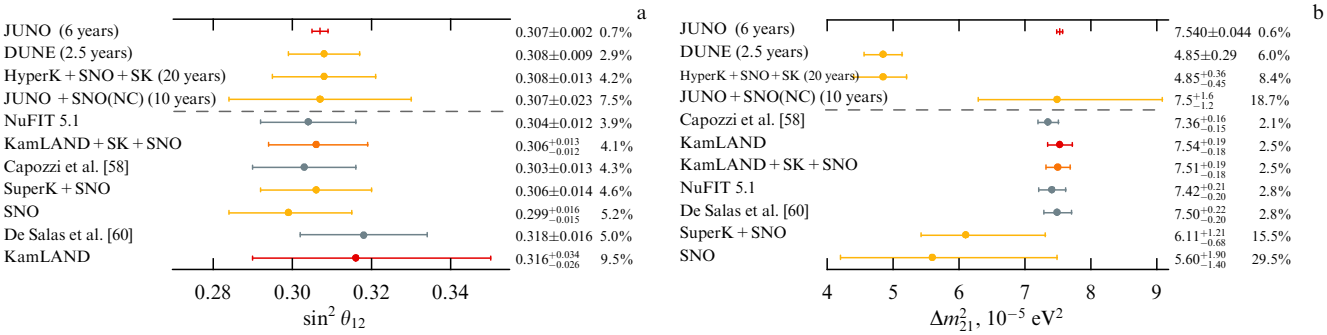

Figure 1. Measured oscillation parameters $\sin^2\theta_{12}$ (a) and Δm^2_{21} (b). Colors show experiment types: red represents reactor experiments, yellow, solar, and orange, a combination of the two types. Dark gray indicates results of global fits. Sensitivities of future experiments are shown above the dashed line for comparison; number in parentheses is the number of years required to achieve the presented accuracy. Different central values of future estimates are due to initially different assumptions regarding values of parameters used in calculating sensitivities. In particular, values for DUNE (Deep Underground Neutrino Experiment) and Hyper-Kamiokande (HyperK) are oscillation parameters that were justifiably relevant at the time sensitivity was evaluated in a joint fit to data of solar experiments [58–63]. (Figure adapted from [64].)

SNO + Super-Kamiokande levels out the preference for the NSI parameters in the $\nu_e \to \nu_e$ ($\overline{\nu}_e \to \overline{\nu}_e$) oscillation channel. This discrepancy may simply be due to a statistical or systematic error.

2.1.2 Mixing angle θ_{13}. Daya Bay [67], Double Chooz [68], and RENO [69] reactor experiments provided an unprecedented high level of accuracy with which the angle θ_{13} was measured. The first experiment to obtain a nonzero value of angle θ_{13} at a 79% confidence level was the KamLAND reactor experiment [70] carried out in 2010. Two accelerator experiments, T2K and MINOS (Main Injector Neutrino Oscillation Search) [71], confirmed in [72, 73] the result in 2011. A year later, the Double Chooz reactor experiment collaboration published in [74] the result of measurements of θ_{13}. However, it should be noted that at that time the statistical significance of individual experimental measurements did not exceed 3σ. Based on all available data, a global fit was performed in 2011 [75], as a result of which the indication of a nonzero θ_{13} increased to $> 3\sigma$.

The first experiment to find a nonzero angle θ_{13}, i.e., to measure a nonzero value at a 5σ confidence level, was the Daya Bay reactor experiment [76], conducted in 2012. Shortly after that, the RENO experiment published results of its measurements [77] with a comparable significance level of 4.9σ. In the subsequent years, the accuracy of the measurement of θ_{13} has increased, and now it is $\sim 3\%$ (Fig. 2). The dominant contribution to the determination of θ_{13} was made by the measurements carried out by Daya Bay and RENO. The Daya Bay experiment completed data collection [83] in 2020, and the final result will be published in the coming years. RENO planned to complete the data set in 2021. Double Chooz completed the physical data set in 2018.

Future experiments will achieve a sensitivity of θ_{13} comparable to that of the reactor experiments of the past decade, but most likely the accuracy level of individual measurements will not be surpassed.

2.1.3 Difference of squared masses $|\Delta m^2_{32}|$. The combined accuracy of determining the difference of squared masses $|\Delta m^2_{32}|$ approaches 1%. This parameter is measured in experiments with accelerator, reactor, and atmospheric neutrinos. The value of the angle θ_{13}, which turned out to be fairly large, enabled the Daya Bay and RENO reactor

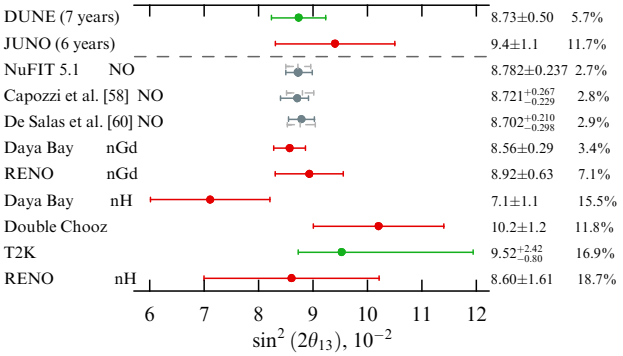

Figure 2. Measured $\sin^2(2\theta_{13})$ values. Colors show experiment types: red represents reactor experiments and green, accelerator experiments. NO is for normal ordering; nGd and nH indicate neutrino capture reactions on gadolinium and hydrogen, respectively. Dark gray color indicates the results of global fits; gray dashed line shows measured values under the assumption of inverted hierarchy. Sensitivities of future experiments are displayed above the dashed line for comparison; number of years required to achieve the indicated accuracy is given in parentheses. Different central values of future estimates are due to initially different assumptions regarding the values of parameters in calculating sensitivities [58–60, 78–82]. (Figure adapted from [64].)

experiments to also measure $|\Delta m^2_{32}|$. The result obtained by Daya Bay is the most precise at the moment. Accelerator experiments (NOvA (NuMI (Neutrinos at the Main Injector) Off-axis ν_e Appearance) [84] and T2K) in recent years have reached reactor sensitivity in determining $|\Delta m^2_{32}|$ and, since Daya Bay and RENO terminated operations, their data will be the most accurate in the coming years, until the launch of next-generation experiments. The current measurements are shown in Fig. 3.

2.1.4 Mixing angle θ_{23}. Another 'atmospheric' parameter, the mixing angle θ_{23}, is measured in experiments with accelerator (NOvA, T2K) and atmospheric (IceCube [94], Super-Kamiokande) neutrinos. Since the angle θ_{23} is close to $\pi/4$, the question remains open: in what octant does its exact value lie? This mixing angle is responsible for the possible symmetry of ν_τ and ν_μ in ν_2 and ν_3. The case of $\mu-\tau$ symmetry was considered, for example, in [95, 96]. The value of θ_{23} and its possible equality to $\pi/4$ were also discussed in application to models of quark–lepton complementarity, for example, [97] and flavor symmetry A_4 [98].

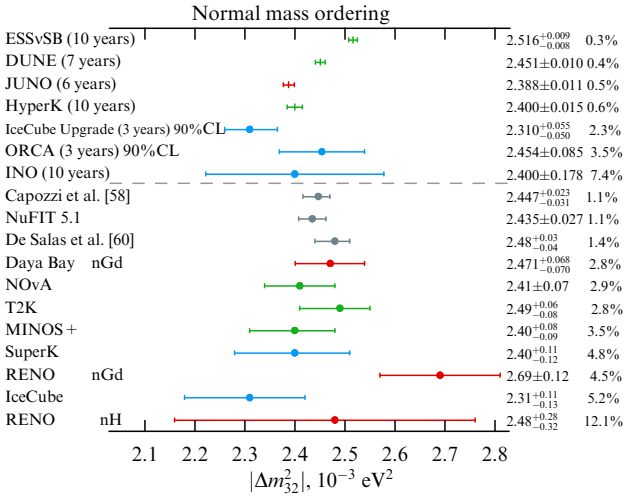

Figure 3. Measured values of $|\Delta m^2_{32}|$ for normal neutrino mass ordering. Colors show experiment types: red represents reactor experiments, green, accelerator, and blue, atmospheric. Dark gray indicates the results of global fits. For comparison, sensitivities of future experiments are displayed above the dashed line; the number of years required to achieve the presented accuracy is indicated in parentheses. Different central values of future estimates are due to initially different assumptions about values of parameters in calculating sensitivities [58–60, 65, 78, 79, 82, 85–93]. (Figure adapted from [64].)

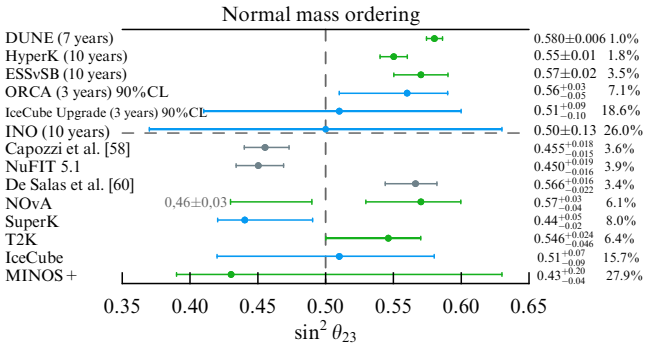

Figure 4. Measured values of $\sin^2\theta_{23}$ for normal neutrino mass ordering. Colors show experiment types: red represents reactor experiments, green, accelerator, and blue, atmospheric. Dark gray indicates the results of global fits. For comparison, sensitivities of future experiments are displayed above the dashed line; the number of years required to achieve the presented accuracy is indicated in parentheses. Different central values of future estimates are due to initially different assumptions about values of parameters in calculating sensitivities [58–60, 65, 78, 79, 85–93]. (Figure adapted from [64].)

Precision measurement of θ_{23} is an urgent and nontrivial task. At the moment, the most probable value of θ_{23}, determined in various experiments, is in the lower octant ($< \pi/4$) θ_{23} (Fig. 4).

2.2 Neutrino mass ordering and the *CP* violation phase

The ordering of neutrino masses is still unknown: $m_1 < m_2 < m_3$ (normal ordering, or normal hierarchy) or $m_3 < m_1 < m_2$ (inverted order, or inverted hierarchy). Therefore, measurements of Δm^2_{32} are experiments that test each of these hypotheses.

Mass ordering, being a basic parameter, the understanding of which requires measuring oscillations of three types of neutrinos, also plays an important role in modeling neutrino fluxes that emerge during the gravitational collapse of stellar nuclei, leading to the formation of supernovae [99]. The flavor composition of neutrinos after passing through high-density stellar matter also depends on mass ordering.

Neutrino mass ordering plays an important role in assessing the prospects for the search for neutrinoless double beta decay [30]. In searching for this process, the sensitivity level of experiments to be attained in the near future will make it possible to detect neutrinoless double beta decay, provided the neutrino mass hierarchy is inverted and this decay takes place. However, if the hierarchy in nature is normal, the development of experimental techniques will be required to increase the sensitivity by several orders of magnitude.

A similar situation occurs in experiments on the direct measurement of neutrino masses and the estimation of $\sum m_{\nu_i}$ from cosmological observations. Namely, in what regards the sensitivity of these experiments, the inverted ordering of neutrino masses is preferable [100]. The mass hierarchy also affects the expected shape of the spectrum in experiments where relic neutrinos are searched for [101].

Given the above reasons, measuring neutrino mass ordering is one of the most challenging tasks of current and future neutrino experiments.

Determining the last unknown parameter — phase δ_{CP} — became fundamentally possible after the angle θ_{13} was measured and turned out to be nonzero (and not very small). The very possibility of measuring the parameter δ_{CP} only appeared in recent years with the launch of a new generation of accelerator neutrino experiments. A fundamental feature of experiments with accelerator neutrinos is the creation of relatively pure beams of particles and antiparticles. To measure the δ_{CP} phase using such beams, the channel in which electron neutrinos ν_e (antineutrinos $\overline{\nu}_e$) are produced must be measured with statistical significance.

Along with the determination of the neutrino mass hierarchy, one of the central tasks of current and future neutrino experiments is to obtain restrictions on the δ_{CP} parameter. The *CP* violation phase δ_{CP} is a potential source of *CP* violation, which is new compared to the quark sector. Some models [102, 103] directly relate *CP* violation caused by the PMNS matrix and baryon asymmetry; for other theories [104, 105], this phase is of no importance.

As noted, the yet unmeasured parameters of the SM lepton sector are the neutrino mass hierarchy, the phase δ_{CP}, and the uncertain value of the mixing angle θ_{23}. Sensitive to the last two parameters, in particular, is the oscillation channel $\nu_\mu \to \nu_e$ ($\overline{\nu}_\mu \to \overline{\nu}_e$), which is used for measurements in current experiments. When a neutrino beam passes through matter, sensitivity to the neutrino mass ordering is involved, since the effect of neutrino interaction with matter is different for the two hierarchies (see Eqn (3)).

Due to the complex dependence of the oscillation probabilities $\nu_\mu \to \nu_e$ ($\overline{\nu}_\mu \to \overline{\nu}_e$) on these three parameters, it is almost impossible to separate the discussion of the actual status of the measurement of *CP* violation and the mass hierarchy. These parameters are currently being measured by the NOvA, T2K, and Super-Kamiokande experiments. In the last experiment, sensitivity to the mass hierarchy appears due to the registration of atmospheric neutrinos and the effect of the interaction of neutrinos with matter on Earth. The sensitivity to δ_{CP} of Super-Kamiokande in the case of atmospheric neutrinos is low due to the low efficiency of separation of electron neutrinos and antineutrinos [106]. After adding in [107] 14 tons of hydrated gadolinium sulfate $Gd_2(SO_4)_3(8H_2O)$ to the water of the Super-Kamiokande

detector, the antineutrino detection efficiency will increase due to an additional signal from neutron capture by gadolinium [108], which will also affect positively Super-Kamiokande's oscillation program. At the moment, the statistical significance of Super-Kamiokande's result is the highest among all experiments. In previous years, the significance level, at which the inverted hierarchy was rejected, was $> 3\sigma$ when globally fitting the data.

In recent years, the preference for the normal hierarchy has been gradually decreasing to reach a significance level of 2.7σ in 2020 according to the results of the NuFIT 5.0 global analysis [109]. A significant role in reducing the preference for the normal mass ordering is played by the disagreement between the results of NOvA and T2K, which has persisted for the past few years. Since both of these projects are currently leaders in sensitivity to the neutrino mass hierarchy and δ_{CP}, the status of NOvA and T2K and the technique for their measurements are presented below in more detail.

The setup of accelerator experiments for studying neutrino oscillations is similar. The T2K experiment began collecting data four years earlier than NOvA, which allowed it to enter the race for obtaining indications of a nonzero mixing angle θ_{13} [110, 111]. The proton synchrotron of the J-PARC (Japan Proton Accelerator Research Complex), a joint project of KEK (Japan's High Energy Accelerator Research Organization) and JAEA (Japanese Atomic Energy Agency) [112], is used to form a neutrino/antineutrino beam in T2K. The accelerator complex, consisting of a linear accelerator (in which the energy is boosted from several keV to 400 MeV), a fast-cycling synchrotron (up to 3 GeV), and the main synchrotron, allows accelerating protons to an energy of 30 GeV and bringing them to a stationary graphite target every 2.5 s. In 2020, a record high beam power of 515 kW was achieved [113] (the experiment facility operates stably at this value), the intensity was 2.5×10^{14} protons per pulse, and the pulse duration was 5 μs.

The NOvA experiment, based at the Fermi National Accelerator Laboratory (FNAL) (Illinois, USA), is funded by the US Department of Energy. As in the T2K project, protons sequentially pass through a chain of accelerators. At the final stage, in the Main Injector synchrotron, they are accelerated to an energy of 120 GeV and also collide with a carbon target. The record high beam power at the moment is 843 kW (average value is 750 kW); the intensity is 5.2×10^{13} protons per pulse, and the beam is output onto the target every 1.3 s.

An important characteristic of collecting statistics in accelerator neutrino experiments is the beam power, which is proportional to the proton beam energy and the number of protons per pulse and inversely proportional to the acceleration cycle time. The operation of accelerator complexes producing neutrino beams, their comparison, and development prospects are considered in detail in review [114]. By shortening the cycle to 1.16 s and increasing the number of protons per pulse to 4.3×10^{14}, J-PARC is expected to reach a beam power of 1.3 MW by 2028. In the FNAL accelerator complex, the cycle time is planned to be reduced to 1.2 s, and the number of protons per pulse to be increased to 7.6×10^{13} (later up to 15×10^{13}). As a consequence, the FNAL beam power will reach 1.2 MW (2.4 MW) by 2026 (> 2030).

Both experiments use the already standard scheme of two — near and far — detectors. The near detector measures the neutrino spectrum when neutrino oscillations make a negligible contribution. The far detector measures the effect of these oscillations. In NOvA and T2K, the detectors are located off the beam axis to obtain a quasi-monochromatic spectrum and suppress high-energy events from the tail of the spectrum, which form the background. The peak energy of the T2K neutrino beam is 0.6 GeV; for NOvA, due to the longer oscillation base, the value of 1.8 GeV was chosen for the energy of the neutrino beam.

2.2.1 T2K experiment detectors. The T2K near detector complex, located at a distance of 280 m from the target, consists of the INGRID (Interactive Neutrino GRID) beam-axis detector and the ND280 facility [20] located at an angle of 2.5° off-axis. INGRID [115] is a sandwich structure assembled from cross-shaped modules. The modules consist of iron planes and a segmented scintillator. Neutrino events are identified by muon tracks, which set the beam direction and profile. An additional module on the beam axis, called the proton module, which only consists of a scintillator, is used to register the quasi-elastic channel of neutrino interactions and compare these data with simulation results.

The detector complex, which is essential for oscillation physics, ND280, located in the same experimental hall but at an angle to the beam, consists of several parts (Fig. 5a):

- P0D detector [116] for measuring the cross section of neutrino interaction with a water target in the neutral current channel with π^0 production;
- tracking detector based on TPC (Time-Projection Chamber) [117];
- two highly segmented scintillation detectors, FGD (Fine Grained Detector) [118];
- electromagnetic calorimeter, ECAL [119], supplementing the internal detectors for complete reconstruction of all events;
- SMRD (Side Muon Range Detector) [120] for detecting muons with large angles of emission with respect to the beam direction, which also operates as a veto system for cosmic muons.

These devices are located inside the magnet of the former UA1 experiment [121], which creates a uniform magnetic field of 0.2 T.

Since 2018, an additional experiment, WAGASCI/Baby-MIND (WAter Grid And SCIntillator detector)/Baby Magnetized Iron Neutrino Detector) [122], has been carried out in the experimental hall of T2K's near detector [122]. In addition to its own physical program, it also fulfills an important task of measuring the ratio of H_2O:CH cross sections of neutrino interactions with water and hydrocarbon targets. This data will facilitate reducing the bias in extrapolating hydrocarbon results to a water target, since the far detector uses water as the active material.

The main task of the near detectors of the long-baseline accelerator experiments is to measure the ν_μ ($\overline{\nu}_\mu$) and ν_e ($\overline{\nu}_e$) fluxes, which will be used to predict the signal events of the disappearance of $\nu_\mu \to \nu_\mu$ ($\overline{\nu}_\mu \to \overline{\nu}_\mu$) and the appearance of $\nu_\mu \to \nu_e$ ($\overline{\nu}_\mu \to \overline{\nu}_e$) and the background $\nu_e \to \nu_e$ ($\overline{\nu}_e \to \overline{\nu}_e$) in the far detector of the experiment. T2K's near detector also makes it possible to reliably measure other backgrounds, for example, the interaction of neutrinos via neutral currents with the production of π^0.

T2K's far detector is a Super-Kamiokande facility located at a distance of 295 km from J-PARC. Some 20 years ago, the Super-Kamiokande experiment, together with the SNO experiment, discovered neutrino oscillations. Super-Kamiokande's Cherenkov detector, which is a cylinder 39 m in

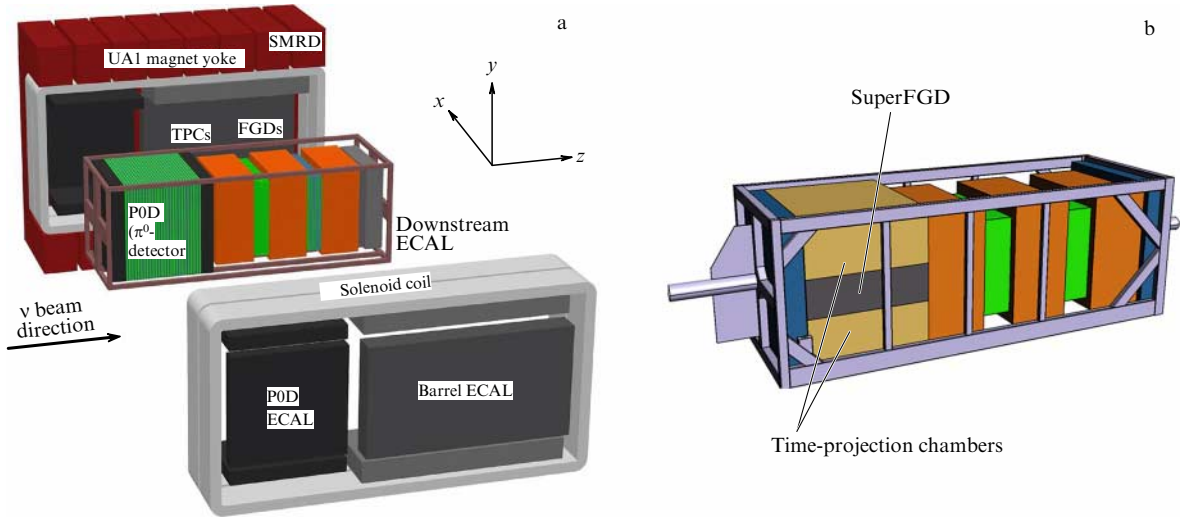

Figure 5. Schematic representation of the ND280 detector complex of the T2K experiment: (a) in the current configuration and (b) upgrade planned for the T2K-II and Hyper-Kamiokande experiments.

diameter and 42 m in height filled with 50 kt of pure water, consists of two parts — internal and external. Events from the internal detector (in which 40% of the surface are geometrically covered with photomultipliers) are used for the physics program. The external detector provides background protection and operates as a veto system for atmospheric muons. Super-Kamiokande can detect atmospheric, accelerator, and solar neutrinos, owing to which its science program is very rich.

2.2.2 NOvA experiment detectors. The near detector of the NOvA experiment, located at an angle of 0.8° to the neutrino beam axis, is a tracking calorimeter assembled from planes consisting of polyvinyl-chloride cells filled with a liquid scintillator. The near detector is located at a distance of 1 km after the graphite target at a depth of 105 m, which protects it from the background of cosmic muons. The size of the near detector is $3.9 \times 3.9 \times 15.9$ m. The far (downstream from the beam) part of the detector contains a muon catcher consisting of steel sheets alternating with scintillator planes.

The NOvA far detector is a liquid scintillation calorimeter of the same design as the near detector, but with larger dimensions, $15.5 \times 15.5 \times 59.6$ m. Planes with alternating x and y directions are located perpendicular to the beam. The cross section of the individual cells, of which the planes are assembled, is the same in the near and far detectors, 6×4 cm, and the cell length is equal to the transverse size of the detectors.

The oscillation base in NOvA is 810 km. The energy resolution for peak energies is 10% for ν_μ ($\bar{\nu}_\mu$) and 11% for ν_e ($\bar{\nu}_e$). A feature of the NOvA experiment is the almost complete equivalence (except for the size) of the near and far detectors, which, in the case of extrapolation, provides a reduction in some of the systematic uncertainties.

2.2.3 Current NOvA and T2K results. Results of measuring the parameters of neutrino oscillations, which were relevant at the time of writing this review, were presented in 2020 at the NEUTRINO 2020 conference [123]. The expected news was the updated results for the mass hierarchy and δ_{CP}. A curious fact was the diminished statistical significance of the previous result of the T2K experiment, published in *Nature* a few months earlier [124]. The reasons were adjustments in Super-Kamiokande calibrations and models of fluxes and cross sections. However, the δ_{CP} value was affected most significantly by the new data collected in 2019–2020, which once again confirms the immense influence exerted on the result by statistical fluctuations and the instability of the model parameters extracted in low-statistic experiments.

The current results are as follows. T2K prefers the normal neutrino mass ordering at the significance level $> 1\sigma$ and $\delta_{CP} = 1.37^{+0.32}_{-0.22}\pi$ [78]. Super-Kamiokande favors the normal hierarchy at the level of 71.4–90.3% obtained by the CLs method [125] and $\delta_{CP} = 1.39^{+0.28}_{-0.44}\pi$ [65]. In the case of NOvA, the preference for the normal hierarchy is at a significance level of 1σ and $\delta_{CP} = 0.82^{+0.24}_{-1.0}\pi$ [93]. Despite the seemingly large differences among the results obtained, the disagreement in terms of the determined δ_{CP} value is not that great: it does not exceed 2σ. This issue is discussed in more detail below.

The current situation, when T2K and NOvA prefer different values of δ_{CP}, due to degeneracy, leads to the fact that joint fitting to the data of both experiments favors the inverted neutrino mass hierarchy [109, 126] (Fig. 6). Whether this is actually due to a statistical fluctuation, an unknown systematic error, or an exotic possibility — a manifestation of new physics — is currently unknown. Due to the specifics of the setups described above, the approaches to taking into account systematic uncertainties and to oscillation analysis in general in the two experiments are significantly different.

For ease of comparison of different components of the analyses of the NOvA and T2K experiments, they are presented below in the form of a step-by-step comparison.

Due to the detectors being identical, NOvA uses the procedure of extrapolation to the far detector of the predictions tuned in the near detector, which are obtained by the Monte Carlo method. It is precisely the components of the predictions in the spectrum that are reweighted based on the reconstructed energy. The impact of each systematic uncertainty is evaluated in the same way: predictions shifted by the amount of uncertainty are tuned in the near detector and then extrapolated to the far one. In the case of NOvA, this extrapolation does not result in a contribution to the error due to different detector materials, a circumstance that

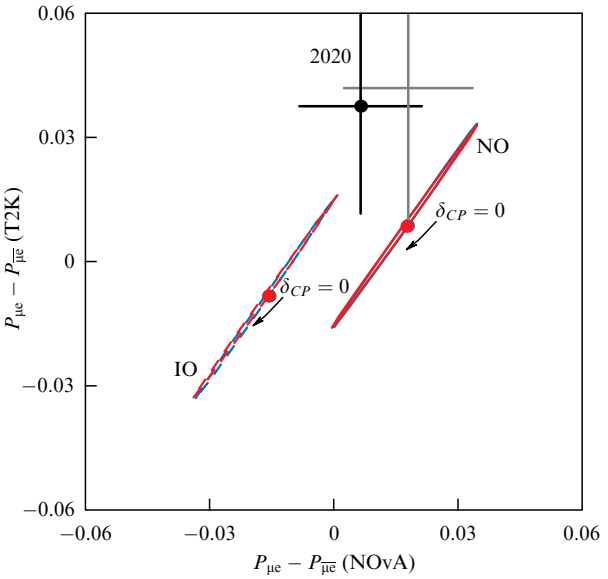

Figure 6. Differences between the probabilities of $P(\nu_\mu \to \nu_e)$ and $P(\bar{\nu}_\mu \to \bar{\nu}_e)$ oscillations for NOvA (abscissa axis) and T2K (ordinate axis) [126]. Solid lines correspond to the normal mass hierarchy; dashed lines correspond to the inverted one. Red curves refer to T2K; blue, to NOvA. If the results of these two experiments are combined, the inverted hierarchy of neutrino masses, $\delta_{CP} = 3\pi/2$, turns out to be preferable. Best fit result is shown with a black dot. Red dots correspond to $\delta_{CP} = 0$. Previous result is shown in gray.

makes it possible to significantly reduce the effect of systematic uncertainties associated with the beam and neutrino interaction cross sections: the total systematic uncertainty of measurement when extrapolation is used is approximately halved. The systematic uncertainties associated with the detector are less controlled during extrapolation. In fitting to far detector data, only adjusted predictions are taken into account. Candidate events are divided into several spectra according to the reconstructed energy: ν_μ ($\bar{\nu}_\mu$), divided into four spectra according to the fraction of the hadron shower energy in the total energy; ν_e ($\bar{\nu}_e$), divided into two spectra depending on the value of the neutrino event classifier. The data analysis itself can be characterized as a frequentist analysis with profiled systematic uncertainties and penalty terms.

Unlike NOvA, T2K detectors are not identical; however, several detector subsystems with water layers described above are available for correct measurements on water. At the moment [127], 18 event groups are used, categorized depending on the topologies registered in the FGD. Data in the near detector are approximated in the space of the parameters (p_μ, $\cos\theta_\mu$), which are well reconstructed in this detector. The ≈ 600 parameters associated with the ND280 detector, ≈ 50 parameters associated with interaction cross sections, and ≈ 100 parameters associated with neutrino fluxes are also varied. In T2K's near detector, it is precisely the parameters of the models used and their uncertainties that are adjusted, due to which the total uncertainty is more than halved compared to the theoretical error.

The updated parameters for the flux and cross section models are used when fitting to far detector data. Marginalization and integration using Monte Carlo methods with Markov chains are used to account for nuisance parameters in the fit [128]. In the far detector, oscillation parameters and about 50 nuisance parameters associated with the systematic uncertainties of the Super-Kamiokande detector are fitted. Five groups of events are used: spectra of candidate events ν_μ ($\bar{\nu}_\mu$), ν_e ($\bar{\nu}_e$), and one new class of events introduced into the analysis [129] in 2017, which is the ν_e-interaction via charged currents with the production of one pion. The last class provides a significant contribution to the significance level of the maximum *CP* violation preference. However, the disagreement between the simulation results and T2K data for this class of events should be noted. An additional artificial increase in the level of significance [130] appears, because the model does not agree with the data even at the best fit point.

The data analysis methods used in T2K are more developed than those in NOvA. This is partly due to the earlier physical start of the experiment compared to that of NOvA. Currently, there are three options for data approximation in T2K: frequentist using the Feldman–Cousins method [131], as in NOvA, purely Bayesian, and hybrid. The Bayesian approach alone uses the simultaneous fitting to the data of both near and far detectors.

Event modeling plays an important role in oscillation analysis. In the case of T2K, due to the lower beam energy, the main class of neutrino interactions is the quasi-elastic interaction, a smaller contribution is due to the resonance channel with the production of one pion and the MEC (meson exchange current) [132] (2p2h) interactions, and the smallest fraction of events is the deep inelastic interaction. The main software employed for modeling neutrino interactions is NEUT[133].

In NOvA, GENIE (Generates Events for Neutrino Interaction Experiments) [134] is used as a generator of neutrino interactions; furthermore, the weights for the cross sections in it are additionally adjusted based on the near-detector data [135]. As a result, due to different interaction generators and different approaches to their tuning, both experiments apply similar modeling of quasi-elastic and resonance interactions, but a different approach to MEC and deep inelastic interactions. However, despite some similarity, the beam energies, selection of events, and energy reconstruction methods in the experiments are different. Therefore, the impact of systematic uncertainties in experiments on the analysis of data is different.

As constraints for flux simulation using the FLUKA software package, T2K uses external constraints from the NA61/SHINE experiment (SPS (Super Proton Synchrotron) Heavy Ion and Neutrino Experiment) [136] at CERN. which measures the hadron yield resulting from a collision of a proton beam with a thin target and with a replica of the T2K experiment target. In addition, the flux is registered in INGRID and muon monitors along the beam path. In NOvA, the neutrino flux is modeled using the GEANT4 software package and adjusted using the PPFX package [137] developed at MINERvA (Main Injector Neutrino Experiment to study ν–A interactions). The latter package uses external data on the production of hadrons in the target from the experiments of Barton et al. [138], NA61, NA49, and MIPP (Main Injector Particle Production). An important potential source of systematic uncertainty here is the adjustment of the NA61 and NA49 systematic errors used by T2K and NOvA, respectively.

Regarding the detectors of the NOvA and T2K experiments themselves, they are different, so the systematic uncertainties associated with them are different and are assumed to be uncorrelated.

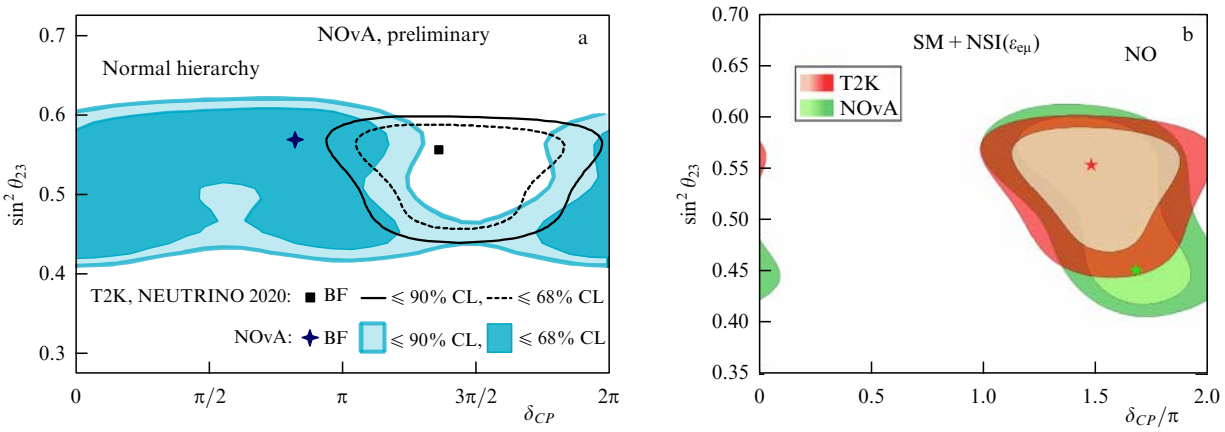

Figure 7. Comparison of confidence contours obtained by NOvA [93] and T2K [78] experiments: (a) in separate analyses without NSI and (b) with NSI parameters obtained by joint fitting to the data of these experiments with NSI [141]. Symbols show corresponding best fit (BF) results. For each experiment, contours of 68% and 90% confidence levels are highlighted in different colors.

Although the difference between the NOvA and T2K results is only $\sim 2\sigma$, an exotic possibility, nonstandard interactions (NSIs) [139], has recently been proposed to explain this discrepancy (Fig. 7a).

Nonstandard interactions were introduced to implement massless neutrino oscillations in matter in the original work by L Wolfenstein [45]. An additional term in the Hamiltonian looks like the following:

$$H = \frac{1}{2E}\left[U^{\dagger}M^2U + a\begin{pmatrix} 1+\varepsilon_{ee} & \varepsilon_{e\mu} & \varepsilon_{e\tau} \\ \varepsilon^*_{e\mu} & \varepsilon_{\mu\mu} & \varepsilon_{\mu\tau} \\ \varepsilon^*_{e\tau} & \varepsilon^*_{\mu\tau} & \varepsilon_{\tau\tau} \end{pmatrix}\right], \qquad (5)$$

where E is the neutrino energy, U is the mixing matrix, M is the diagonal matrix of squared mass differences, $a = 2\sqrt{2}G_{\rm F}N_{\rm e}E$ is the term responsible for the interaction of neutrinos with matter, and $N_{\rm e}$ is the electron density. The terms $\varepsilon_{\alpha\beta}$ are the parameters characterizing the magnitude of the new interaction relative to the weak interaction, arising from the effective Lagrangian. For the neutral current, they are defined as

$$\mathcal{L}_{\rm NSI} = -2\sqrt{2}G_{\rm F}\sum_{\alpha,\beta,f}\varepsilon^f_{\alpha\beta}(\bar{\nu}_\alpha\gamma^\mu\nu_\beta)(\bar{f}\gamma_\mu f)\,. \qquad (6)$$

The NSI parameters in the Hamiltonian and Lagrangian are related as follows: $\varepsilon_{\alpha\beta} = \sum_f (N_f/N_{\rm e})\varepsilon^f_{\alpha\beta}$, where N_f is the concentration of fermions. For matter on Earth, it can be assumed that $N_{\rm n} \simeq N_{\rm p} = N_{\rm e}$, in this case $N_{\rm u} \simeq N_{\rm d} \simeq 3N_{\rm e}$: $\varepsilon_{\alpha\beta} \simeq \varepsilon^{\rm e}_{\alpha\beta} + 3\varepsilon^{\rm u}_{\alpha\beta} + 3\varepsilon^{\rm d}_{\alpha\beta}$.

Studies [140, 141] explore the hypothesis of complex NSI $\varepsilon_{\alpha\beta} = |\varepsilon_{\alpha\beta}|\exp(i\phi_{\alpha\beta})$ via neutral currents. NSIs may be a low-energy manifestation of the high-energy physics of new heavy states or may be associated with light mediators.

Since the NSI effect is directly related to the interaction of neutrinos with matter, it is of interest to compare the results of experiments with different bases or different types of matter, and the differences among their results may be an indirect indication of the presence of NSI. Coupling constants $\varepsilon_{e\mu}$ and $\varepsilon_{e\tau}$ are considered, potentially related to the oscillation probabilities $\nu_\mu \to \nu_e$. For the $\mu-\tau$-sector corresponding to $\nu_\mu \to \nu_\mu$ strong restrictions are available, which follow from atmospheric experiments [142, 143]. In the presence of NSI, joint fitting to the T2K and NOvA data results in a value of leptonic $\delta_{CP} \sim 3\pi/2$ and a preference for the normal hierarchy (Fig. 7b). For phases $\phi_{e\mu}$ and $\phi_{e\tau}$ of new interactions, the maximum *CP* violation is also preferred. In the case of the inverted hierarchy, where NOvA and T2K are mutually consistent, no signs of NSI are found. The best fit for NOvA + T2K in the presence of NSI $|\varepsilon_{e\mu}| = 0.19$ [140], which is not strongly rejected by the IceCube analysis $|\varepsilon_{e\mu}| = 0.07$ (Fig. 8) given the accuracy of the analysis performed. The result of the second group [141] for this parameter, $|\varepsilon_{e\mu}| = 0.15$, is within 90% of IceCube CL [144, 145].

Also, one of the possible explanations for the discrepancy between the results of NOvA and T2K is the violation of Lorentz invariance. It was shown in [146] that, if this hypothesis is true, the discrepancy between the results of NOvA and T2K is slightly reduced. In [147], possible nonunitarity of the Pontecorvo–Maki–Nakagawa–Sakata mixing matrix is considered. In [148], the running neutrino masses and mixing parameters are hypothesized, which also implies new physics manifesting itself in quantum corrections. In the presence of these effects and taking into account the limitations from short-baseline experiments, the discrepancy between NOvA and T2K is slightly smoothed out. It has also been shown that sterile neutrinos cannot explain this disagreement [149].

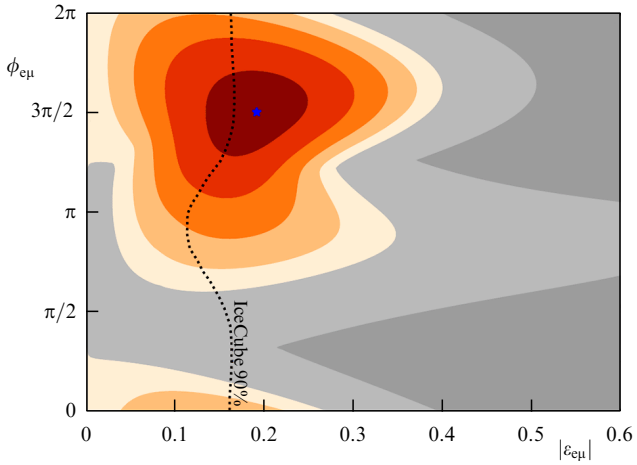

Figure 8. Confidence contours on the NSI parameter plane $\varepsilon_{e\mu}-\phi_{e\mu}$ in a joint fit to the data of NOvA and T2K experiments [140]. Orange contours correspond to the step $\Delta\chi^2 = 1$. Gray areas are excluded by NOvA and T2K results. Dotted curve shows the constraint on these parameters obtained by the IceCube experiment.

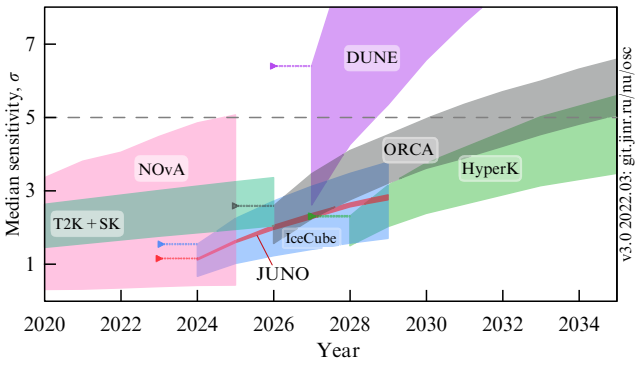

Figure 9. Expected sensitivity of ongoing and future experiments to the neutrino mass hierarchy by years. Figures of different colors represent areas of possible measurement, limited by combinations of oscillation parameters, which lead to extreme sensitivity values for each experiment. Triangles mark the beginning of data collection.

Despite interesting possible interpretations of the obtained results, the statistical significance of the disagreement is small. A number of improvements are expected in NOvA and T2K in the coming years. The modernization of the J-PARC and FNAL accelerator complexes for Hyper-Kamiokande and DUNE involves staged improvements that also affect currently running experiments. Owing to this, T2K will gain 200×10^{20} POT (Protons On Target) by ~ 2026, which will increase sensitivity to maximum *CP* violation up to 3σ. The near detector will be upgraded to play an important role in the future Hyper-Kamiokande experiment. These changes will be discussed in Section 3.

The expected improvements in NOvA will mainly affect the FNAL accelerator complex and data analysis. By the end of data collection in ~ 2025, the beam power from the accelerator will be 900 kW (the design power is 700 kW). Currently, a prototype test-particle beam detector at Fermilab [150] is collecting statistics, which will improve the understanding of detectors and their response. Consequently, the corresponding systematic uncertainties will decrease.

Figure 9 shows the expected NOvA and T2K sensitivities in measuring the neutrino mass hierarchy with a breakdown by years. By the launch of Hyper-Kamiokande and DUNE, the mass hierarchy will most likely be measured at a significance level of $3-4\sigma$. In the case of the maximum *CP* violation phase, the sensitivity to rejection $\delta_{CP} = 0, \pi$ is 3σ at best for the T2K experiment and $\sim 2\sigma$ for NOvA.

Of interest is also the future first full-fledged joint analysis of T2K and Super-Kamiokande data, similar to the analysis of data with accelerator and atmospheric neutrinos following the example of MINOS [151]. Study [152] showed a slight improvement in the sensitivity of Super-Kamiokande if the results published by T2K are used. A full-fledged joint analysis of the NOvA and T2K experiments [153] is also scheduled for 2022.

3. Prospects

3.1 Future accelerator experiments

The NOvA and T2K experiments will collect data until 2025–2026, until the accelerator facilities are stopped for the final preparatory work for the Hyper-Kamiokande and DUNE experiments.

3.1.1 Hyper-Kamiokande. By 2022, in the T2K experiment as part of T2K-II program [154], it is planned to complete the upgrade of the near detector, which will also be used in the Hyper-Kamiokande project. The current design of the ND280, as described in Section 2, is optimal for detecting particles moving in the direction of the neutrino beam, primarily charged leptons and neutral pions. The far Cherenkov detector features a good particle detection efficiency at all lepton emission angles. Thus, the acceptance of the near detector is much less than that of the far one. In addition, the threshold for the detection of pions and protons in the near detector is high, while neutrons are mostly not detected. The design also has a number of restrictions on the efficiency of reconstruction, energy and time resolution, and identification of secondary particles moving in a plane perpendicular to the direction of the primary neutrino or scattered in the opposite direction.

Phase II upgrades consist in the replacement of the P0D with a high-precision, highly segmented SuperFGD scintillation detector [155] and the deployment of two horizontal time-projection chambers [156] and a time-of-flight detector [157] around this new tracker (Fig. 5b). The total mass of the active part of the detector will almost double, up to 4 t, which will lead to a significant increase in the number of detected events.

The $2 \times 2 \times 0.6$ m SuperFGD consists of approximately two million 1 cm^3 polystyrene cubes isolated from each other by reflective walls. The light signal is transmitted to the photodetector via an optical fiber passing in three perpendicular projections and through all the cubes to the side walls of the detector. The three-side signal readout, combined with the top and bottom surroundings of the two time-projection chambers, allows high-resolution 3D reconstruction of tracks and showers, while detailed segmentation also allows reconstruction of fast neutron tracks for better reconstruction of antineutrino energy. The efficiency of muon detection will reach $\sim 70\%$ at emission angles of $\sim 90^\circ$, while in the previous version of the detector it was practically zero. The proton detection efficiency is assumed to be $\sim 90\%$ for momenta > 400 MeV/c. The expected efficiency of neutron detection is 60%, and the energy resolution is 15–30%. Temporal resolution of SuperFGD is 950 ps, and that of the time-of-flight detector is 150 ps. The minimum requirement for the new ND280 TPCs is to provide the same physical capabilities as the current P0D, but in a smaller volume. The new chambers will use argon-based gas and Micromegas resistive detectors.

Preliminary tests have shown an improvement in key performance, especially in spatial resolution: it is now three times better (< 200 μm at 10 cm drift) than in the current P0D detector. It is expected that, due to the modification of the P0D detector described above, the total systematic error will decrease from 5–6% to 3–4%. For the T2K-II experiment, the reduction in systematic uncertainty does not play a significant role, since experiments of the current generation are limited by statistical error. On the contrary, for the Hyper-Kamiokande experiment, the modernization of the ND280 and the reduction in systematic uncertainty are of utmost importance for solving primary physical problems.

Hyper-Kamiokande's far detector [158], a water Cherenkov detector with a target mass of 258 kt, is a cylindrical container 68 m in diameter and 71 m high; its fiducial volume is 188 kt, eight times that of Super-Kamiokande. Hyper-Kamiokande, like Super-Kamiokande, will use 20-inch

photomultiplier tubes (PMTs) with 40% geometric coverage as photodetectors. The detector will be located inside Mount Nijugoyama in the Tochibora mine in Kamioka at a distance of 295 km from the J-PARC accelerator complex (and about 8 km south of Super-Kamiokande). The neutrino flux will be directed at an angle of 2.5° off the beam axis, as in the T2K experiment. The research program of Hyper-Kamiokande is even more vast than that of Super-Kamiokande: the detection of accelerator, atmospheric, solar, and geoneutrinos, the exploration of proton decay and other rare processes, the registration of a neutrino signal from supernovae, etc.

In addition to the near and far detectors, it is planned to install an intermediate water Cherenkov detector (IWCD) [159] with a target mass of about 1 kt, located at a distance of about 1 km from the target in J-PARC. The water tank will be able to move vertically and scan the energy spectrum of the neutrino beam with various values of the off-axis angle. The IWCD target is completely identical to the Hyper-Kamiokande target, which, in turn, will enable taking into account and reducing the systematic uncertainties of the oscillation analysis associated with the neutrino interaction cross section to a significant extent.

3.1.2 DUNE. Another megascience project is the international DUNE experiment [160]. The concept of this experiment for measuring neutrino oscillations is similar to that of NOvA: the muon neutrino flux is generated using the accelerator complex based at Fermilab. This full-scale project includes a number of improvements to the existing infrastructure implemented at Fermilab. The LBNF (Long Baseline Neutrino Facility) project [161] includes the creation of a separate output of the proton beam from the Main Injector Synchrotron in the direction of South Dakota, the entire infrastructure for producing a neutrino beam, and experimental halls for detectors located at Fermilab and the Sanford Underground Research Facility (SURF) in Lead (South Dakota, USA).

PIP-II [162] is a continuation of the PIP (Proton Improvement Plan) [163] project to increase the intensity of the proton beam of the accelerator complex at Fermilab, which was launched in 2012. PIP and PIP-I + basically have already been implemented [164] for NOvA, MINERvA, and earlier for MINOS/MINOS + . This stage of improvement only consisted in the optimization of existing accelerators without any major upgrades. Due to the implementation of PIP and PIP-I + , the NOvA beam power will be able to reach about 1 MW in the coming years. According to the PIP-II plan for DUNE, the main improvement is the replacement of the 400-MeV linear accelerator with a normal conductivity with an 800-MeV superconducting accelerator, which will make it possible to achieve a power of 1.2 MW with a beam energy of 120 GeV. PIP-II should be completed in 2025–2026; a further increase in proton beam power for DUNE to 2.4 MW (intensity $(1.1-1.9)\times 10^{21}$ POT yr^{-1}), according to the PIP-III plan [165], can be achieved by replacing the booster and upgrading the new linear accelerator and Main Injector Synchrotron. Since DUNE, unlike Hyper-Kamiokande, is planning a significant change in the design of the experiment, its optimization to achieve the main goal is ongoing, and a number of characteristics and parameters are still being discussed. For example, the proton beam energy has not yet been chosen; therefore, in all refereed sources, a possible range of 60–120 GeV is reported. The final

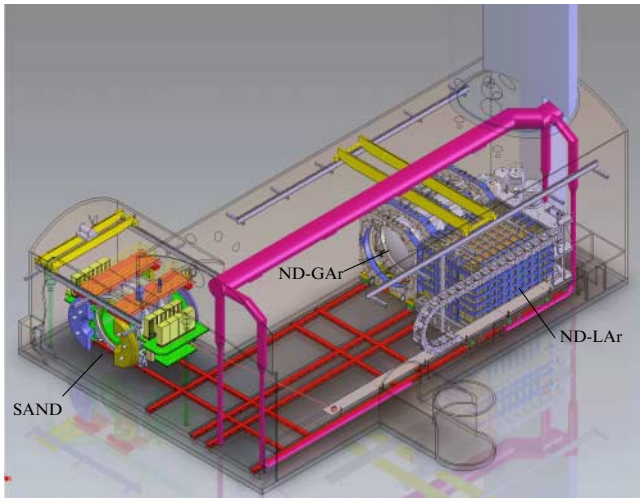

Figure 10. Setup of DUNE's near detectors at Fermilab.

choice will be based on increasing the sensitivity of the experiment to the measurement of oscillation parameters. The main characteristics of the beam line are also optimized to solve the main physical problem of the experiment. Part of the infrastructure under development, except for the target and magnetic horns, cannot be changed in the future. For example, the length of the decay channel for mesons affects the resulting neutrino spectrum: with increasing length, the number of high-energy neutrinos increases, while an increase in diameter, on the contrary, yields more lower-energy neutrinos. An excessively long channel will increase the background of neutrinos with the wrong sign of the lepton number[3] and the number of electron neutrinos/antineutrinos initially present in the beam.

According to the LBNF project, the system of near detectors DUNE-ND (Fig. 10) [166] will be located in Fermilab in an experimental hall with dimensions of 30×17 m at a depth of ≈ 60 m at a distance of 574 m from the target. The multicomponent system of near detectors includes a modular liquid argon time projection chamber (LArTPC) called ND-LAr, an ND-GAr facility consisting of a high-pressure gas time projection chamber (GArTPC), and an electromagnetic calorimeter; it also contains a neutrino beam detector-monitor (System for on-Axis Neutrino Detection, SAND) and a mechanized mobile platform that enables positioning these detectors at various angles relative to the beam, the so-called DUNE–PRISM (Precision Reaction-Independent Spectrum Measurement) system.

The working substance of the main near detector for oscillation physics, the liquid argon time projection chamber, is identical to that of the modules of the experiment's far detector, which will reduce some of the systematic uncertainties. The main task of this detector is to measure the spectra from the interaction of neutrinos on argon prior to oscillations and to predict the spectra ν_μ ($\overline{\nu}_\mu$) and ν_e ($\overline{\nu}_e$) in the far detector. A common cryostat will house a modular structure of 35 time-projection chambers with a system for detecting the charge and scintillation light emerging in argon [167]. The signal from this structure will be used as a time stamp to reconstruct events in several modules and eliminate overlaps

[3] Admixture of neutrinos in an antineutrino beam and vice versa.

(so-called pile-ups) of events that occur during beam spill and to improve energy resolution by registering the part of the energy converted into light.

Efficient use of the DUNE–PRISM system requires the same energy resolution of the near and far detectors, currently expected at a level of 15–20% for the total neutrino energy, depending on its flavor. The main contribution to this value comes from the energy resolution of the hadron shower ($> 30\%$). The expected number of charged current ν_μ events in the detector per year reaches 10^8 on the beam axis.

The total dimensions of the ND-LAr detector, 7×3 m across the beam and 5 m along it, make it possible to detect muons with a momentum up to 0.7 GeV/c. To increase this range, it is proposed to place downstream from the ND-LAr the ND-GAr facility; the latter consists of a GArTPC chamber in a magnetic field of 0.5 T with an Ar:CH_4 (9:1) working gas at a pressure of 10 bar and an electromagnetic calorimeter of alternating layers of scintillator and copper. This setup will allow recording the momentum of muons emitted from the LArTPC and distinguishing the charge of leptons, which will make it possible to provide good control over the background of neutrinos with the wrong sign of the lepton number. The GArTPC design is largely inspired by the time projection chamber of ALICE (A Large Ion Collider Experiment), while the magnetic system reproduces that of the NICA/MPD (Nuclotron-based Ion Collider fAcility/ Multi-Purpose Detector) experiment [168] at the Joint Institute for Nuclear Research (Dubna).

Due to the complexity of the ND-GAr design, an option is being discussed to place a temporary muon spectrometer (TMS) instead of it, to be replaced later by a GArTPC detector.

Both detectors, with liquid and gaseous argon, will be located on a mobile platform, which will make it possible to carry out measurements both on the axis of the neutrino beam and off the beam (the DUNE–PRISM concept). The platform can be displaced to a distance of up to 33 m. A wide energy spectrum on the beam axis ranging from 0.5 to 8 GeV with a maximum in the region of 2.5 GeV spans two oscillation maxima. When shifted to the maximum off-axis distance (angle $\approx 2.5^\circ$), the peak occurs at a value of 0.5 GeV. Such beam scanning makes it possible to significantly reduce the systematic uncertainties associated with the neutrino beam and the cross sections of neutrino interactions.

Another DUNE-ND detector at Fermilab, SAND, will be fixed on the beam axis to monitor the neutrino flux, especially when ND-LAr and ND-GAr are displaced off axis (up to 50% of full exposure). The detector design includes a solenoidal superconducting magnet with a field of 0.6 T, an electromagnetic calorimeter from KLOE (K LOng Experiment) (Frascati, Italy), a new internal track detector based on straw tubes (STT option (Straw Tube Tracker)), and a thin liquid argon target. The option to place layers of polypropylene and carbon between the STT system modules is being considered, which will make it possible to separate neutrino interactions on hydrogen using the $CH_2 - C$ subtraction method [169].

For a long time, the only measured cross sections of neutrino interaction with hydrogen were provided by low-statistics bubble chamber experiments. By comparing the cross sections for hydrogen and argon, it is proposed to reduce the uncertainties in calculations of neutrino interactions associated with nuclear effects. SAND with the STT tracker, in addition to studies of importance for oscillation physics, will make it possible to carry out other measurements.

The DUNE far detector will be located in the underground SURF center at a depth of ≈ 1.5 km and at a distance of 1300 km from the target at Fermilab. The detector will consist of four liquid argon time projection chambers (LArTPCs) with a mass of 10 kt. A decision has been made on the first two modules, which will be single phase with vertical and horizontal drift. The published sensitivity estimates for the experiment assume a single-phase technology for all four modules, which does not take full advantage of modules with different detector technologies and, as a result, different systematic uncertainties. Each module is a structure measuring $13.3 \times 12 \times 58$ m, divided longitudinally into four drift volumes. The mass of the active part of the detector is 13 kt; currently, the selection criteria cut out a fiducial volume of 10 kt. The far detector, unlike NOvA, T2K, and Hyper-Kamiokande, will be used to conduct research on the axis of the neutrino beam and thus increase the number of statistics of events, measure a wide range of neutrino energies, and be able to span two oscillation maxima. Due to its design, DUNE can efficiently separate the signal from backgrounds, especially from events with interactions via neutral currents.

An interesting idea is the Theia project [170], which is considered one of the modules of the DUNE far detector. Theia is a water-based scintillation detector with a mass of 25 kt [171] that can detect both Cherenkov and scintillation light. The components can differ in wavelength [172], time, and angular distribution. The presence of a scintillator will lower the threshold for detecting particles to ~ 1 MeV, which is fundamentally important for detecting solar neutrinos and the diffuse background of neutrinos from supernovae.

The potential of a long-baseline accelerator experiment is already clear from the experimental setup (Fig. 11). In accelerator beam measurements, DUNE's oscillation base is

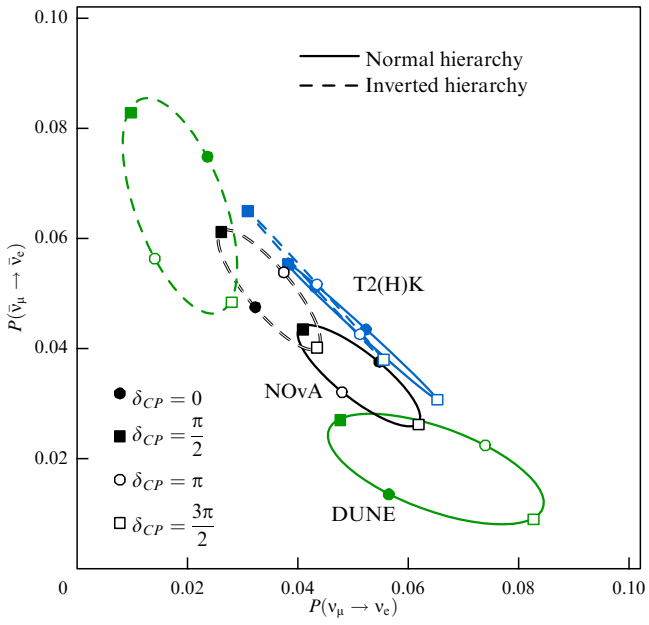

Figure 11. Probabilities of $P(\nu_\mu \to \nu_e)$ and $P(\bar{\nu}_\mu \to \bar{\nu}_e)$ oscillations in matter in NOvA, T2K (Hyper-Kamiokande), and DUNE accelerator experiments for different values of δ_{CP} and both types of neutrino mass hierarchy. Overlapping of regions for the same experiment implies degeneracy of the parameters.

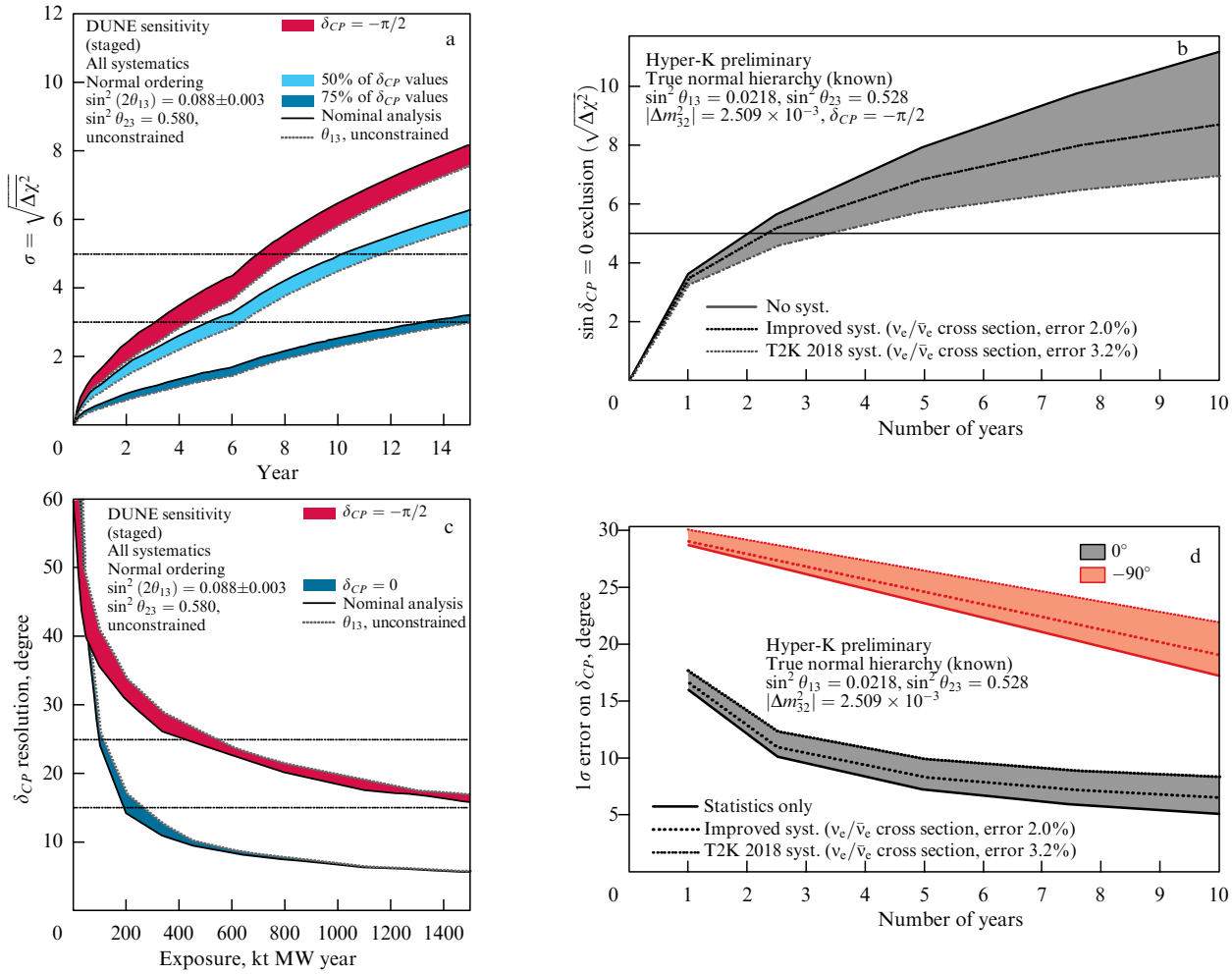

Figure 12. Expected sensitivities of DUNE and Hyper-Kamiokande (Hyper-K) in the measurement of δ_{CP} for different years of experiments. Significance levels with which DUNE (red curve) (a) and Hyper-K (b) reject the hypothesis $\delta_{CP} = 0, \pi$ with the value realized in nature $\delta_{CP} = 3\pi/2$. Resolution of the measurement of δ_{CP} for the cases $\delta_{CP} = 0$ and $\delta_{CP} = 3\pi/2$ for experiments DUNE (c) and Hyper-K (d). Set of statistics 2.7×10^{21} POT in Hyper-K (Fig. b, d) was calculated for a beam of neutrinos and antineutrinos at a 1:3 ratio.

larger than that of Hyper-Kamiokande. As a consequence, due to the greater effect of the interaction of neutrinos with matter, sensitivity to the neutrino mass hierarchy is enhanced. A potentially interesting option is the greater sensitivity to NSI due to the larger baseline [173, 174]. Due to the degeneracy of δ_{CP} with a mass hierarchy, a large base of oscillations can confuse both measurements. However, it was shown in [175] that these two parameters are distinguishable for an oscillation base exceeding 1200 km.

Lately, the sensitivity of an experiment in which δ_{CP} is measured has been conventionally represented in terms of its ability to reject the values $0, \pi$ corresponding to *CP*-parity conservation in the case of the maximum phase value $(3\pi/2)$ (Fig. 12a, b). This sensitivity focuses on the single value of δ_{CP}, which quite possibly is not implemented in nature. More informative, in our opinion, is the accuracy with which δ_{CP} is measured, rather than the exclusion of individual points. The expected resolution values of DUNE and Hyper-Kamiokande are presented in Fig. 12c, d. Figure 9 shows the expected sensitivities for measuring the neutrino mass hierarchy in Hyper-Kamiokande, DUNE, which are discussed.

The Hyper-Kamiokande detector, like DUNE, can detect atmospheric, accelerator, and solar neutrinos. To measure the mass hierarchy and phase δ_{CP} in Hyper-Kamiokande, a joint analysis of data on atmospheric and accelerator neutrinos will be carried out. Atmospheric neutrinos are more sensitive to the mass hierarchy, while accelerator ones are more sensitive to δ_{CP}, and joint fitting of both data types improves the final sensitivity. The major reported estimates of DUNE sensitivity have been made exclusively for the accelerator neutrino beam. The sensitivity to mass hierarchy with DUNE atmospheric neutrino detection alone reaches 3σ over seven years of data collection. Based on the Hyper-Kamiokande example, it can be expected that the use of atmospheric neutrinos will improve the sensitivity of the experiment in the joint analysis of data from different sources.

The Hyper-Kamiokande accelerator beam provides high sensitivity to phase δ_{CP}, but only provided the mass hierarchy is known. It is quite possible that by the time DUNE and Hyper-Kamiokande start operations, global data analysis will reach the value of 5σ in favor of some mass ordering. However, according to current expectations (see Fig. 9), the measurement of the neutrino mass hierarchy is precisely a task for the next generation of experiments. Therefore, it is possible that DUNE and Hyper-Kamiokande will have to concurrently measure both parameters: the mass hierarchy and δ_{CP}.

An interesting extension of the Hyper-Kamiokande experiment was the proposal to place an additional detector

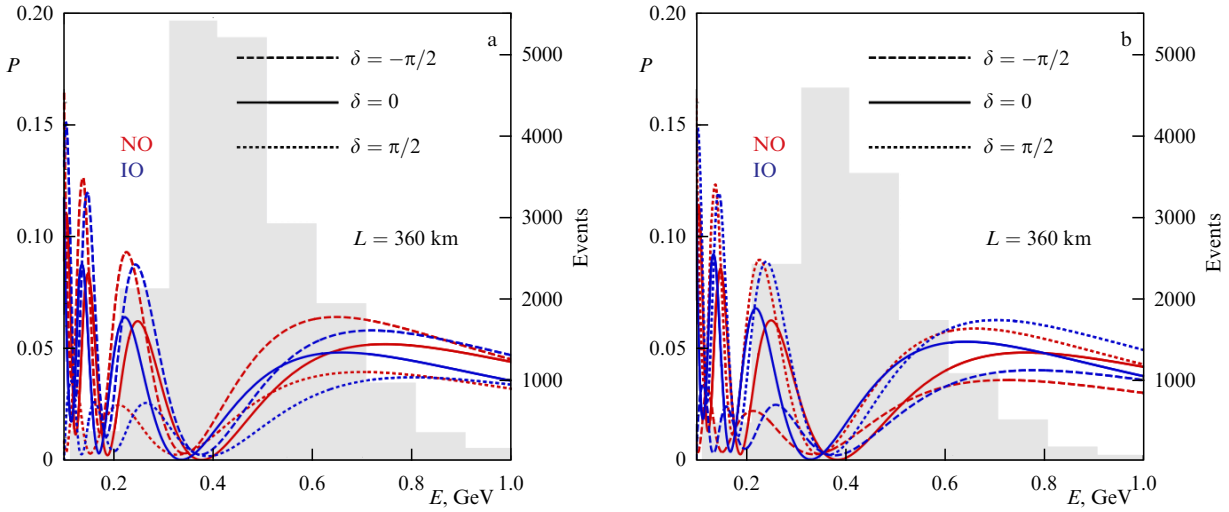

Figure 13. Concept of the second oscillation maximum illustrated by the example of the ESSνSB experiment for a baseline of 360 km: a beam of neutrinos (a) and antineutrinos (b). *P* is the probability of oscillations. Gray color represents the histogram of predicted events in arbitrary units. Oscillation maxima are numbered from right to left.

in Korea [176], which would increase the oscillation base to 1000–1200 km, depending on the location. Theia was also proposed as a detector. However, the status of this proposal is currently unclear.

The approaches of the DUNE and Hyper-Kamiokande experiments are complementary [177] due to different setups and techniques. Their most important task will be to cross check the results obtained.

Due to the registration of neutrinos from different sources, both DUNE and Hyper-Kamiokande will be able to refine 'solar' and 'atmospheric' parameters of oscillations in addition to performing the main tasks: measuring δ_{CP} and determining the hierarchy of neutrino masses. Owing to new intense beams, accelerator experiments will become the leaders in measuring the former in the coming years. For example, over seven years, DUNE will be able to measure $\sin^2\theta_{23}$ with an accuracy of 1% and Δm^2_{32} at 0.4%. The sensitivities of future experiments are presented more clearly and in detail in Figs 1, 3, and 4. Regarding the measurement of $\sin^2(2\theta_{13})$ in accelerator experiments, the expected sensitivity is currently known only for DUNE (see Fig. 2), which over 15 years of data collection will reach the measurement accuracy of Daya Bay.

3.1.3 ESSνSB. The future long-baseline accelerator neutrino program is mainly concentrated at Fermilab (USA) and J-PARC (Japan). The previous European long-baseline experiment with a neutrino beam from CERN to the Gran Sasso laboratory, OPERA (Oscillation Project with Emulsion-tRacking Apparatus) [178], was completed in 2012, having experimentally registered for the first time $\nu_\mu \to \nu_\tau$ oscillations at a level $> 5\sigma$ [179]. A new European accelerator experiment, ESSνSB (European Spallation Source Neutrino Super Beam) [180], may appear on the map of the oscillation accelerator neutrino program, but plans for this project have not yet been finalized.

The ESSνSB setting is similar to that of Hyper-Kamiokande, and its physical tasks are the same. The main advantage of this experiment is a very intense neutrino flux due to a proton beam with a power of 5 MW and an energy of 2 GeV from a linear accelerator [181] of a pulsed neutron source (ESS, European Spallation Source) (Sweden), which corresponds to 2.4×10^{23} POT yr^{-1}.

The near detector [182], like that of Hyper-Kamiokande, will consist of several parts: a 1.7-kt water-Cherenkov detector as the main part, a track detector (Super Fine-Grained Tracker) with a magnetic field for studying the cross sections of neutrino interactions, and an emulsion detector with layers of water and iron, like NINJA (Neutrino Interaction research with Nuclear emulsion and J-PARC Accelerator) [183], to study the topology of events.

The far detector, based on the concept of MEMPHYS (MEgaton Mass PHYSics) [184], will have two modules with a mass of 373 kt each, and its neutrino and antineutrino energy resolution will be 10–20%.

Currently, two locations of the far detector are being considered: at distances of 360 or 540 km [185]; the beam energy will be chosen in a range of 200–600 MeV, depending on the base, to cover the second oscillation maximum, where the value of $P(\nu_\mu \to \nu_e) - P(\overline{\nu}_\mu \to \overline{\nu}_e)$ is three times greater than in the first maximum. For the second oscillation maximum, the influence of systematic errors weakens [186], but the number of signal events also decreases due to the larger base and smaller cross section. The probabilities of neutrino and antineutrino oscillations for ESSνSB with a 360-km baseline, on which both the first and second oscillation maxima[4] are partially covered, are shown in Fig. 13.

In addition, the ESSνSB experiment setup will make it possible to measure the 'atmospheric' parameters of neutrino oscillations with high accuracy (see Figs 3 and 4). Data for the determination of 'solar' parameters are not yet available. The sensitivity of the ESSνSB experiment is only reported for the accelerator neutrino beam, but, by analogy with Hyper-Kamiokande, physical results can be expected with both solar and atmospheric neutrino fluxes.

All the above accelerator experiments are based on obtaining a neutrino beam from the decay of mesons as a result of a collision of a proton beam with a fixed target.

[4] Due to a broad spectrum, DUNE can reliably detect both the first and the second maximum.

Features of this method are contamination of the beam with other neutrino flavors and a wide range of energies. Interesting alternative methods are neutrino factories [187], beta beams [188], and DAR (Decay At Rest) experiments. Experiments based on the first and last methods are currently ongoing. Neutrino factories are based on the idea of accumulating muons and using them to produce a beam of neutrinos. Such a beam will consist of muon and electron neutrinos in equal proportions and with different signs of the lepton number. The main problem with this approach is the need to accumulate a large number of muons. The νSTORM (Neutrinos from STORed Muons) experiment [189] at CERN is a prototype of this idea. The DAR technique, which was used in the LSND (Liquid Scintillator Neutrino Detector) [190] and KARMEN (KArlsruhe Rutherford Medium Energy Neutrino experiment) [191] experiments, have been recently tested in the MiniBooNE (Mini Booster Neutrino Experiment) [192] with kaon decay at rest. The JSNS^2 (J-PARC Sterile Neutrino Search at J-PARC Spallation Neutron Source) [193, 194] and IsoDAR (Isotope Decay-At-Rest experiment) [195] experiments with decays of muons and ions at rest, respectively, are also planned.

Another CERN project that aims to explore alternative methods for obtaining neutrino beams is ENUBET (Enhanced NeUtrino BEams from kaon Tagging) [196]. The idea is to label an electron or positron produced in the decay of a kaon through the K_{e3} channel, which is virtually the only source of electron neutrinos in the beam ($\sim 97\%$). In this way, the neutrino energy can be reconstructed from kinematics. Due to the detection of leptons after passing through the decay channel, the beam of muon neutrinos from pion decays can also be accurately reconstructed. This option is currently under consideration by the ENUBET collaboration. The neutrino tagging technique was previously tested in the KMN (Russian abbreviation for Tagged Neutrino Complex) experiment [197] in Protvino (Russia) in the 1980s–2000s and was recently proposed for the P2O project (Protvino–ORCA) [198].

3.2 Future reactor experiments

Detecting reactor electron antineutrinos in long-baseline experiments is a completely independent way to determine the neutrino mass hierarchy with its own advantages and disadvantages. Currently, this class of experiments is only represented by the JUNO (Jiangmen Underground Neutrino Observatory) project with a baseline of 53 km, which is at the stage of detector assembly; its completion is scheduled for 2023.

Reactor electron antineutrinos are produced in beta decays of nuclear fission products, primarily ^{235}U, ^{239}Pu, ^{238}U, and ^{241}Pu [199], and are detected in the inverse beta decay $\bar{\nu}_e + p \to e^+ + n$ with an energy threshold of about 1.8 MeV. The characteristic energies of the observed electron antineutrinos, which do not exceed 10 MeV, are insufficient for the production of heavier leptons and, accordingly, for the observation of other flavor states. Thus, reactor experiments only observe the survival probability of electron antineutrinos given by Eqn (4).

The measured quantities are represented in the observed spectrum in a nondegenerate way, and they can be extracted from the data with little correlation with other oscillation parameters. The hierarchy of neutrino masses manifests itself in the interference of terms of Eqn (4) proportional to $\sin^2(2\theta_{13})$. The sensitivity to the neutrino mass hierarchy is the highest for reactor antineutrinos at a distance of about 53 km. The corresponding spectrum of detected particles is shown in Fig. 14.

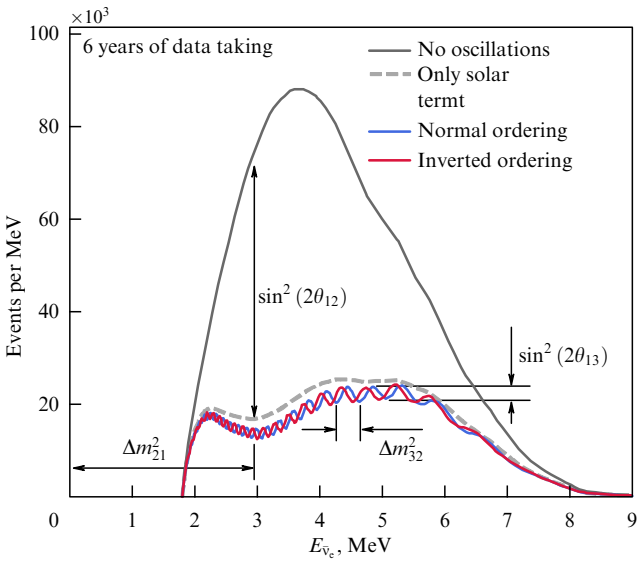

Figure 14. Spectrum of reactor electron antineutrinos expected at JUNO [200], which corresponds to six years of data collection, assuming a normal (blue curve) and inverted (red curve) hierarchy. Spectrum of antineutrinos without oscillations being taken into account (dark gray curve) is marked, and the influence of each oscillation parameter is shown.

The main detector of the JUNO experiment is an acrylic sphere 35 m in diameter [201] filled with 20 kt of a liquid scintillator (Fig. 15). Approximately 17,500 20-inch PMTs [202] and 25,600 3-inch PMTs will be mounted on a steel structure surrounding the acrylic sphere. The experiment will observe the flux of antineutrinos from six nuclear reactors operated at the Yangjiang nuclear power plant (NPP), with a thermal power of 2.9 GW each, and two reactors of the Taishan NPP, with a thermal power of 4.6 GW each [203]. All these reactors are located at a distance of about 53 km from the detector, and their total thermal power is 26.6 GW. The experiment will observe about 45 antineutrino interactions[5] per day at a background level of 8.6% [204, 205]. With statistics of about 100,000 events collected over six years, JUNO will be able to determine the hierarchy at a significance level of 3σ [205].

The JUNO experiment will measure the neutrino oscillation parameters Δm^2_{21}, $\sin^2(2\theta_{12})$, and Δm^2_{32} with an accuracy of 0.6% (see Figs 1b, 1a, and 3, respectively). The accuracy of measuring the mixing angle $\sin^2(2\theta_{13})$ will not reach the level of accuracy of modern reactor experiments with an intermediate baseline. It should be noted that the accuracy of measuring the solar parameters Δm^2_{21} and $\sin^2(2\theta_{12})$ dominant measurement. The measurement accuracy Δm^2_{32} will reach that of the best experiments.

Since the determination of the neutrino mass hierarchy in JUNO is associated with the resolution of small oscillations in the antineutrino spectrum, of critical importance is the ability of the detector to reconstruct the positron energy, from which the neutrino energy is approximately determined. To do so, the energy resolution σ_E/E should be no worse than 3% for a released energy of 1 MeV [202], and the nonlinearity of the

[5] This estimate takes into account that only two reactors of the initially planned four will be commissioned at the Taishan NPP [204].

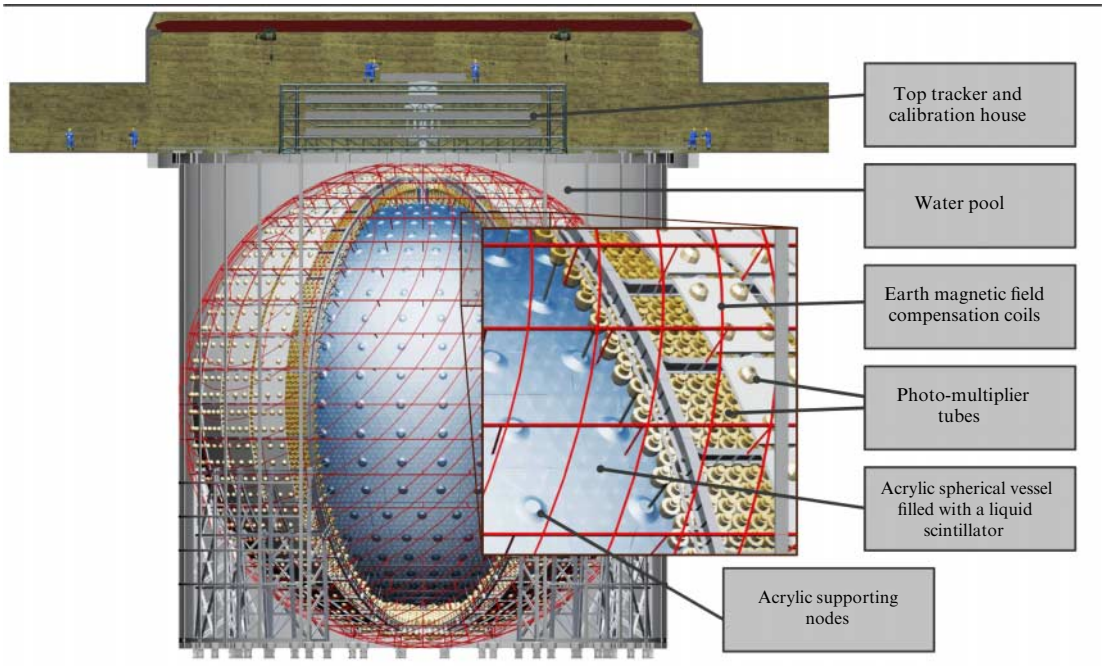

Figure 15. Schematic representation of the JUNO detector [200].

energy scale should be no worse than 1%. Such record-setting characteristics are achieved by enhancing the light collection: the geometric coverage of the PMT detector is $\sim 75.2\%$ [205], the high quantum efficiency of the PMT is $\sim 30\%$ [202], and of the light yield of a liquid scintillator is optimized [206].

Another challenge for the JUNO experiment is the prediction of the reactor antineutrino spectrum. Currently existing models of the antineutrino spectrum [207–209] are known to be plagued with a significant systematic error, conservatively estimated at 5% for conversion spectra and 20% for spectra determined by the summation method [210]. Due to the high uncertainty of the spectra obtained by the summation method, now the antineutrino spectrum [207] from ^{235}U, ^{239}Pu, and ^{241}Pu fissions, which make the main contribution to the antineutrino flux from the reactor, is used as a reference. The reactor antineutrino spectrum [207] was obtained from the conversion of beta spectra measured at Institut Laue–Langevin (ILL) in the 1980s [211, 212].

For antineutrinos originating from ^{238}U fission, for lack of better data, the spectrum [208] determined by the summation method is used. The spectrum estimated in this way features deviations from the experimental one, which are conventionally divided into two probably unrelated classes. First, the antineutrino flux from the reactor shows a total statistically significant deficit of about 5% [213], which is called the 'reactor antineutrino anomaly.' In 2021, measurements of the ratio of the beta spectra of ^{235}U/^{239}Pu [215] showed that the beta spectrum from ^{235}U measured at ILL is overestimated by 5%. Taking into account the resulting correction reduces the significance of the reactor anomaly from two standard deviations to one [216]. The remaining disagreement can also be explained by the transition of the neutrino due to oscillations to a sterile state with a mass on the order of 1 eV [217].

Second, a local excess is observed in the flux of reactor antineutrinos in the energy range from 4.8 to 6.8 MeV in all intermediate-baseline experiments [218–220]. This deviation, called the 5-MeV 'bump,' is sometimes also referred to as the five-MeV shoulder or excess. The reasons for the appearance of the shoulder include incorrect prediction of the ^{241}Pu spectrum (summation method) [210], differences in the energy spectra of thermal neutrons in ILL (conversion) and reactors [210], and the shape of the spectrum of forbidden decays in the conversion process not being taken into account [214, 221].

Some studies [222, 223] predict the presence of a fine structure in the reactor antineutrino spectrum. The fine structure is related to the Fermi correction to the spectra of individual electrons and antineutrinos produced in beta decay, which leads to a sharp cutoff of the antineutrino spectrum. When the spectra of a large number of beta decay chains are added together, a sawtooth structure appears with an amplitude of the order of several percent and a characteristic scale of the order of several ten keV. Such a structure will not be visible in modern reactor experiments, but may affect the sensitivity of JUNO, as it will interfere with the observed oscillations in the spectrum.

To date, the spectrum of reactor antineutrinos has been measured with the best accuracy in the Daya Bay and RENO experiments [219, 224], but their measurements are limited by the energy resolution σ_E/E of the detectors, which is about 7–8% at an energy of 1 MeV. Therefore, a satellite detector, TAO (Taishan Antineutrino Observatory) [203], will be built at JUNO to accurately measure the antineutrino spectrum. The TAO detector will be installed at a distance of 30 m from one of the Taishan NPP reactors. The TAO is intended to measure the antineutrino spectrum with an energy resolution σ_E/E of 2% per MeV. A spherical detector with a diameter of 1.7 m will be filled with 2.6 tons of a gadolinium-doped liquid scintillator. Light will be collected by silicon PMTs covering about 94% of the detector surface. To reduce dark noise from the Si PMTs, the detector will be placed in a cryostat at an operating temperature of $-50\,^{\circ}$C. The TAO will be able to observe about 2000 antineutrino interactions per day. Should data be collected for at least three years, the detector will collect statistics on about 2 million events and measure the

spectrum of reactor antineutrinos with a statistical uncertainty of 1%.

Thus, while in accelerator experiments the determination of the hierarchy is complicated by the dependence on δ_{CP} and $\sin^2\theta_{23}$, the main challenge for JUNO is of an instrumental nature and associated with the need to provide a sufficiently high energy resolution. Like other projects that use large detectors, JUNO is a multi-purpose experiment, the physics program of which also includes the detection of solar neutrinos of low [225] and high [226] energies, the detection of geoneutrinos [205] and atmospheric neutrinos [225], the possible detection of neutrinos from bursts of supernovae and the diffuse neutrino flux from supernovae, and the search for proton decay.

Measurements of oscillation parameters in JUNO are also related to the possibility of detecting solar and atmospheric neutrinos. The JUNO detector will observe daily about 17 electron neutrinos [226] produced in ^{8}B decay in the Sun with energies ranging from zero to ~ 14 MeV, detected via elastic scattering on electrons. Solar neutrinos with similar energies undergo the MSW effect when passing both the Sun's matter and through Earth when detected at nighttime. Interaction with solar matter distorts the observed neutrino spectrum. The influence of the terrestrial environment manifests itself primarily as a flux variation within 2%, depending on the zenith angle.

Within 10 years, JUNO will be able to detect day/night asymmetries at a level of three standard deviations and to measure the 'solar' mass squared difference Δm^2_{21} with an uncertainty of 20% (Fig. 1b). The measurement of Δm^2_{21} in JUNO using neutrinos from two different sources will shed light on the disagreement between the measurements of the squared mass difference in the KamLAND and Super-Kamiokande + SNO experiments mentioned above. The value of $\sin^2\theta_{12}$ will be measured at JUNO with an external flux limit from the SNO data over the neutral current channel and will achieve an accuracy of 8% (Fig. 1a). The main challenge in this measurement is to achieve a signal-to-background ratio of ~ 2. To this end, it is planned, first, to develop efficient algorithms for suppressing the cosmogenic background and, second, to achieve a high radiation purity of the scintillator: the content of ^{238}U and ^{232}Th should not exceed 10^{-17} g g^{-1} for each isotope. To monitor the radiation purity at the JUNO filling stage, it is planned to use an additional liquid scintillation detector, OSIRIS (Online Scintillator Internal Radioactivity Investigation System) with a weight of 17 tons. After making some modifications to improve the energy resolution, reduce the radiation background, and increase the accuracy with which the location of a signal is reconstructed, the OSIRIS calibration detector will be able to operate as a stand-alone experimental facility (under the proposed name SERAPPIS (SEarch for RAre PP-neutrinos In Scintillator) [227]) to detect solar neutrinos from the pp reaction.

The JUNO experiment will detect ν_μ/ν_e ($\overline{\nu}_\mu/\overline{\nu}_e$) oscillations of atmospheric neutrinos in the energy range from 0.1 to 10 GeV. Neutrinos are subject to the effect of interaction with matter that depends on the path passed in Earth's interior, i.e., on the zenith angle. At present, the response of the detector to atmospheric neutrinos has been little studied, so the estimate of sensitivity to the mass hierarchy depends on assumptions about JUNO's ability to distinguish between neutrino flavors, differentiate particle from antiparticle, and reconstruct the direction of a neutrino. In the pessimistic case, with an energy resolution of $5\%/\sqrt{E_{\rm vis}}$, an angular resolution of $37.2^\circ/\sqrt{E_{\rm vis}}$, and the ability to only differentiate events with muon tracks from events with electromagnetic and hadronic showers, JUNO will be able to achieve sensitivity to the neutrino mass hierarchy at a level of one standard deviation (1σ) for 10 years [204]. If ν_μ ($\overline{\nu}_\mu$) events can be distinguished from ν_e ($\overline{\nu}_e$) by the detection of a Michel electron, the sensitivity to the hierarchy can reach the level of 1.8σ. These estimates were obtained under the assumption of $\sin^2\theta_{23} = 0.5$. JUNO's sensitivity to the octant of θ_{23} does not exceed 1σ (0.5σ) for the normal (inverted) hierarchy for the range of θ_{23} values from 40° to 50°. The sensitivity to *CP* violation, δ_{CP}, does not exceed 0.15σ when the neutrino mass hierarchy is known.

It is worth noting that the combined analysis of the neutrino mass hierarchy, including reactor, accelerator, and atmospheric neutrinos, based on data from various sources, provides a sensitivity higher than that resulting from naive statistical summation, which does not take into account the correlation of parameters [228]. The combined sensitivity of JUNO, taking into account the results obtained from the analysis of reactor and atmospheric neutrinos, has not yet been evaluated, but it can be expected that the combined sensitivity to the mass hierarchy will be no worse than $(4-4.5)\sigma$.

A combined analysis of data obtained by JUNO and IceCube Upgrade enables determination of the neutrino mass hierarchy at a level no worse than 5σ over a period of 3–7 years [229], and should data from JUNO and PINGU (Precision IceCube Next Generation Upgrade) be combined, the same sensitivity can be achieved in one and a half (three) years for normal (inverted) hierarchy. In the case of a JUNO and ORCA combination, this accuracy can be achieved within two (six) years for the normal (inverted) hierarchy [92].

A similar enhancement of sensitivity can also be expected from a combined analysis of data from JUNO and accelerator experiments. A simplified model [228], in which data from accelerator experiments are added to the statistics by means of a penalty term for the $|\Delta m^2_{32}|$ value, indicates that by combining data from JUNO, T2K, and NOvA a sensitivity of 5σ can be achieved within six years of data collection.

3.3 Future atmospheric experiments

3.3.1 IceCube. The IceCube neutrino observatory at the South Pole has the opportunity to engage in oscillation physics in addition to implementing an incredibly successful astrophysical program [34, 35, 230, 231]. The interior of this cubic-kilometer Cherenkov detector, DeepCore, is designed to detect events with an energy lower than the rest of the setup [94]. IceCube's main detector, located in the ice at a depth of 1450–2450 m, consists of 78 strings with digital optical modules attached to them with a step of 17 m. The distance between the strings is 125 m. Due to this arrangement of the detection modules, the detection threshold for IceCube is 50–100 GeV, and particles with an energy of about 1 TeV are optimally detected. To register atmospheric neutrinos in the inner part of the detector at a depth below 2100 m, a volume with a radius of 250 m and a length of 350 m, which is called DeepCore, contains more densely spaced strings. Usual IceCube strings alternate with a set of eight strings with a higher density of optical modules (7 m); the distance between the strings in this area is approximately 75 m. Six out of eight strings have new optical modules with a photomultiplier quantum efficiency of 35%. The distance between the strings

in this part of the detector is 42 m. The detection threshold for atmospheric neutrinos in DeepCore is ~ 5 GeV. The rest of the detector operates as a veto system for oscillation physics in DeepCore.

It is noteworthy that, despite the instrumental volume of the IceCube detector of 1 km^3, the confidence volume, taking into account the veto and the efficiency of event selection, is 400 Mt [230], and, taking into account the ice density, the effective volume is 0.44 km^3. The astrophysical experimental facility Baikal-GVD (Baikal Gigaton Volume Detector) [232, 233], located in Russia, with similar tasks and setup, due to the properties of water as a medium for the passage of particles, can provide a larger effective volume than IceCube. If the veto system is not used in the experiment, as is currently planned, the effective volume of the detector may virtually coincide with the instrumental volume (this will also depend on the particle selection efficiency for analysis). For 2021, the instrumental volume of Baikal-GVD, which consists of eight clusters, is 0.45 km^3. Until 2025, it is planned to install 15 clusters, which will increase the total volume to ~ 0.8 km^3. A similar neutrino telescope with a volume of several cubic kilometers, P-ONE (Pacific Ocean Neutrino Experiment) [234], is being deployed in Canada on the basis of the ONC (Ocean Networks Canada) oceanographic observatory. Baikal-GVD and P-ONE have not yet made public their plans to study neutrino oscillations, so they are not considered in more detail here.

IceCube, as an oscillation experiment, is rather limited in research due to the current setting. Since the threshold is high, only a part of the atmospheric neutrino spectrum that is sensitive to oscillations is recorded. The effect of interaction with matter, which is sensitive in atmospheric experiments to neutrino mass ordering, manifests itself in the energy range of 2–10 GeV, a significant part of which is cut out by the high threshold of the detector. An oscillation-focused analysis of IceCube data is carried out for two types of events — track and cascade. The spectrum of the former primarily consists of ν_μ ($\overline{\nu}_\mu$) events in the detector, while the spectrum of the latter is a mixture of all flavors and types of interactions. The detector cannot reliably identify a lepton in the final state. Data are fitted in both spectra in the form of 2D histograms $(E_\nu, \cos\theta)$. Due to this formulation of the problem, the main results of IceCube in terms of oscillation parameters are the measurement of θ_{23} and $|\Delta m^2_{32}|$. The IceCube sensitivity to measuring the neutrino mass hierarchy is low. Nevertheless, research in this area is conducted to obtain important evidence that such a measurement is possible at subsequent stages of the experiment [235].

An interesting result of IceCube is the measurement of the atmospheric ν_τ flux with a search for its possible excess over the expected one [236] within the three-flavor paradigm. Previous measurements of this quantity in the Super-Kamiokande and OPERA experiments (at a level of 1.47σ [237] and 0.25σ [179], respectively) were discussed in connection with possible uncertainty in the ν_τ interaction cross section. Exotic mechanisms have also been proposed, including the nonunitarity of the neutrino mixing matrix due to nonstandard interactions and the existence of sterile neutrinos. It should be noted that, in contrast, IceCube observed a deficit of ν_τ.

Currently, preparations are underway for a new phase of the experiment, IceCube-Gen2 [238, 239]. The installation of new parts of the detector will begin in 2024; throughout the entire modernization, the facility will collect data also using newly commissioned units. Basically, the changes concern the astrophysical program of the experiment. In addition to 78 strings with a distance of 125 m between each pair, 120 new strings will be added with a distance between them of 240 m and new optical modules located every 16 m. As a result, the instrumental volume will increase to 7.9 km^3. On the surface above each string, a station [240] with an antenna and Cherenkov and scintillation detectors will be deployed, forming a ground array to detect cosmic rays similar to that in IceTop. The Cherenkov detector will be complemented by an adjacent radio telescope spanning an area of 500 km^2. Radio emission arises in a medium during the passage of particles with near-light velocities (the Askar'yan effect [241]). Each of the 200 separate stations of which the detector consists will comprise a ground part and underground antennas located at a depth of 100 m. The described modification will enable the event statistics to be increased by an order of magnitude and the angular resolution to be enhanced by a factor of three. As a result, the sensitivity to the source of astrophysical neutrinos will increase fivefold compared to the current one. An additional radio telescope will extend the accessible energy range from a few GeV to about 1 EeV.

An intermediate phase between IceCube and IceCube-Gen2 will be IceCube Upgrade [242], whose strings will also be a prototype for the Gen2 stage. Seven new strings will be added to the DeepCore area with a distance between modules along a string of 3 m, and the final horizontal gap will be 20 m. The facility will be commissioned approximately in 2022–2023. The main improvement consists of increasing the number of statistics of neutrino events in the energy range sensitive to oscillations up to 10 GeV and lowering the event detection threshold to ~ 1 GeV. It is assumed that it will be possible to reconstruct ν_e events with an electromagnetic cascade, which will provide additional sensitivity to the neutrino mass hierarchy. All oscillation channels in the $(E_\nu, \cos\theta)$ plot differ for the two types of mass hierarchy, the effect of which is exhibited in a suppression or enhancement of transitions for various energies and angles. However, some of these differences are too subtle to be seen by a detector with a realistic energy resolution. The improvement in event reconstruction in IceCube Upgrade is an important step in solving this problem.

An improvement in IceCube-Gen2 essential for oscillation physics was supposed to be PINGU [243], another DeepCore segment equipped with even denser strings, with 26 strings in total. As is currently known, the PINGU most likely will not be implemented [244], so it is not discussed here in detail.

3.3.2 ORCA. The oscillation program is an interesting addition to and extension of the astrophysical program of another experiment, KM3NeT (Km^3 Neutrino Telescope) [245]. The KM3NeT project is conceptually a successor of the ANTARES experiment (Astronomy with a Neutrino Telescope and Abyss environmental RESearch) [246], which is also located in the Mediterranean Sea and measures atmospheric and astrophysical neutrinos. KM3NeT will consist of two clusters intended for different tasks: ARCA (Astroparticle Research with Cosmics in the Abyss) [247] and ORCA (Oscillation Research with Cosmics in the Abyss) [245]. The ARCA detector is designed to study high-energy neutrino astrophysics on a TeV–PeV scale, offshore Capo Passero (Italy). Part of KM3NeT, called ORCA, located in the Mediterranean Sea, offshore Toulon (France), will

measure oscillation parameters for atmospheric neutrinos. Both installations are water Cherenkov detectors, very similar to IceCube and Baikal-GVD.

ARCA will consist of two clusters of 115 strings each with optical modules spaced every 36 m. The average distance between the strings is ≈ 90 m. Both clusters add up to an instrumental volume of 1 km^3.

ORCA will consist of a single block containing 115 strings with a distance of 20 m between them and a distance of 9 m between PMTs. The experiment is optimized for measuring atmospheric neutrino oscillations in the energy range of 3–30 GeV. The instrumental volume of the detector is 7 Mt of sea water (a cylinder with a radius of 106 m and a height of 200 m). The angular resolution of ORCA is less than 8° for neutrinos with energies above 5 GeV. The energy resolution is about 20%.

Another interesting development of the ORCA program could be the accelerator neutrino beam originating from Protvino [248], which is produced using the U-70 proton synchrotron. The oscillation baseline in this case will be 2595 km. The beam features a wide spectrum with an average energy of 5 GeV. In this case, the experiment will operate at the first oscillation maximum and be more sensitive to the neutrino mass hierarchy than to δ_{CP}. The beam intensity can be increased from 90 to 450 kW, which is directly related to the planned exposure. Due to the large volume of ORCA, the number of statistics can reach 4000 events per year with a power of 450 kW. The neutrino mass hierarchy can be determined at the $(4-8)\sigma$ significance level after a year of operation with a power of 450 kW or five years of operation with a power of 90 kW. After three years of operation with a 450-kW beam power, the sensitivity to the absence of *CP* violation being excluded can reach 2σ. A challenge is that the flavors of neutrino events cannot be reliably determined, except for ν_μ ($\overline{\nu}_\mu$), which is well identified due to the long track. No plan for implementation of the project is currently available. Another improvement in the ORCA detector under discussion, which is called Super-ORCA [249], is the addition of strings, which will result in their denser (by a factor of 10) arrangement. This will improve the detector's ability to identify the neutrino flavor and lower the detection threshold to values < 1 GeV. With ORCA and a 450-kW accelerator beam from Protvino, the resolution for δ_{CP} measurements can be 10° (16°) for $\delta_{CP} = 0$ ($\pi/2$) after 10 years of data collection.

3.3.3 ICAL to INO. Another experiment planned to explore atmospheric neutrinos is ICAL (Iron CALorimeter) [250] based at the INO (Indian Neutrino Observatory) underground observatory (India). It is located at a depth of 1300 m, where the background level from atmospheric muons is similar to that in the underground laboratory Gran Sasso (Italy). The status of the construction of the INO laboratory, however, is unclear, as the project has slowed down since the decision to establish it was made in 2014.

The structure of the ICAL detector is similar to that proposed in the early 2000s for the MONOLITH (Massive Observatory for Neutrino Oscillation or Limits on THeir existence) experiment [251] at Gran Sasso. It is proposed to use a detector with a total mass of 50 kt, consisting of layers of magnetized iron and a resistive plate chamber (RPC) with a time resolution of 1 ns, which makes it possible to distinguish particle directions. Due to the detector's magnetic field of 1.5 T, it is possible to separate particles and antiparticles, which will make it possible to measure the effect of interaction with matter for neutrinos and antineutrinos and to check the *CPT* invariance. The operating energy range of the detector is 1–10 GeV, while the muon momentum resolution is 10–20%, and the accuracy of determining the zenith angle is on the order of 1°. With these parameters, the experiment is sensitive to oscillations $\nu_\mu \to \nu_\mu$, $\overline{\nu}_\mu \to \overline{\nu}_\mu$, $\nu_e \to \nu_\mu$, and $\overline{\nu}_e \to \overline{\nu}_\mu$, and the main task of the experiment is to determine the neutrino mass hierarchy, measure atmospheric oscillation parameters, and study the effect of interaction with matter, including testing the NSI hypothesis. The detector is virtually insensitive to δ_{CP} and thus helps to avoid degeneracy in combined analysis with experiments sensitive to this parameter.

The sensitivities to the measurement of the neutrino mass hierarchy in accelerator, reactor, and atmospheric experiments are compared in Fig. 9. The abundance of projects in atmospheric oscillation physics is due to the wide possibilities for carrying out measurements with intense natural fluxes of atmospheric neutrinos of different flavors and large variable distances and energies. However, some purely atmospheric neutrino experiments are inferior in terms of sensitivity and implementation time to experiments with artificial sources.

4. Conclusion

Over the past 20 years of experimental studies of the physics of neutrino oscillations, as a result of a number of unique projects, the understanding of this phenomenon has advanced fairly far. Pontecorvo's idea, which turns 65 in 2022, has provided an excellent insight for studying the properties of the neutrino as an elementary particle and exploring the limits of applicability of the Standard Model.

The development of detector technologies provides an opportunity to implement even more ambitious projects, which should definitely clarify the remaining unresolved issues in measuring the oscillation parameters of three types of neutrinos. Due to the immense volume, innovative techniques, the ability to work with several neutrino sources, and the employment of high-intensity artificial beams, next-generation facilities will feature unprecedented sensitivity to measuring neutrino mass ordering (see Fig. 9), the *CP*-parity violation phase in the lepton sector δ_{CP} (see Fig. 12), and the refinement of other parameters. Concurrent measurement with multiple sources will also provide an opportunity to check the unitarity of the mixing matrix.

In this review, we made an attempt to present the current status of the measurement of neutrino oscillation parameters and the prospects related to future projects with a long baseline of oscillations that are sensitive to the last unmeasured parameters: neutrino mass ordering and the phase of *CP* violation δ_{CP}. Joint efforts of completed and ongoing experiments made it possible to increase the accuracy of measuring mixing angles θ_{12}, θ_{23}, and θ_{13} to 4%, 3%, and 3%, respectively, and the squared mass differences, Δm^2_{21} and Δm^2_{32}, to 3% and 1%. It is expected that the future accelerator experiments DUNE and Hyper-Kamiokande will measure δ_{CP} at a high level of accuracy and, together with the JUNO reactor experiment and atmospheric IceCube and KM3NeT experiments, will finally determine the neutrino mass ordering.

In more detail, by 2030–2035, the accuracy of measuring the 'solar' and 'atmospheric' parameters will reach a sub-percentage level. JUNO, which will have high sensitivity to

θ_{12} and Δm^2_{21}, will enable the disagreement between KamLAND and Super-Kamiokande + SNO measurements to be eventually resolved. The long-baseline accelerator experiments DUNE and Hyper-Kamiokande have the highest predicted sensitivity to θ_{23} and Δm^2_{32}. It is expected that in the next few years the mass-squared difference Δm^2_{32} will also be measured in the JUNO experiment with an accuracy that is superior to that of current experiments. After the launch of the DUNE accelerator experiment, the neutrino mass hierarchy will be measured in this experiment at a significance level $> 5\sigma$ within 2–3 years. The JUNO, ORCA, IceCube-Upgrade, and Hyper-Kamiokande experiments are also highly sensitive to the neutrino mass hierarchy. The parameter most difficult to measure, the phase of *CP* violation in the lepton sector, will be the goal of the DUNE and Hyper-Kamiokande experiments. The expected sensitivities for this parameter are highly dependent on the value of δ_{CP} implemented in nature and on the accuracy with which all other parameters will be measured. For individual points, the expected resolution of the experiments to measure δ_{CP} is less than 10°.

Addition at proofreading

After the review had been written and accepted for publication, some results were updated. Nevertheless, it is worth noting that the conclusions drawn in this review remain valid even with new measurements taken into account. The NOvA collaboration published a paper [252], also presenting the result of a reanalysis of the same data using the Bayesian approach [253]. The physical conclusions, however, have not changed. The T2K experiment reported a result [254] which agrees with that presented in this review. A possible explanation of the disagreement between the results of NOvA and T2K due to very light sterile neutrinos was proposed [255]. Updated sensitivities of JUNO [256, 257] and ESSνSB [258] have been published. At the Neutrino-2022 conference [259], a number of updated experimental results were presented, including those of IceCube [260], Super-Kamiokande [261], and RENO [262]. A comparison of actual results and experimental sensitivities can be found at the website [64]. Report [263] presents the project of the European Super-Chooz reactor experiment aimed at studying the same physics as the Daya Bay experiment. Among the interesting papers published in 2022, it is worth noting the final oscillation analysis of Daya Bay data with complete statistics [264], the first measurement of reactor neutrinos with $E > 9$ MeV [265], and the calculation of the oscillation probabilities using a quantum computer [266]. A representative selection of papers [31, 267, 268] appeared, in which neutrino studies are discussed in the context of other physical phenomena.

Acknowledgments

The work on Sections 1 and 2 was supported by the Russian Science Foundation (project 18-12-00271-P). The work on Section 3 was supported by the Ministry of Science and Higher Education of the Russian Federation (contract 075-15-2020-778) as part of the program for financing major scientific projects of the Science national project. The authors are grateful to N V Anfimov, Yu M Malyshkin, A V Stepanova, O Yu Smirnov, K A Treskov, and A V Chukanov for discussing various aspects of this work, and to D V Naumov for careful reading of the draft review and fruitful discussions of all the details.

References

1. Pontecorvo B *Sov. Phys. JETP* **6** 429 (1958); *Zh. Eksp. Teor. Fiz.* **33** 549 (1957)
2. Pontecorvo B *Sov. Phys. JETP* **7** 172 (1958); *Zh. Eksp. Teor. Fiz.* **34** 247 (1957)
3. Bilenky S M *Phys. Usp.* **57** 489 (2014); *Usp. Fiz. Nauk* **184** 531 (2014)
4. Pontecorvo B *Sov. Phys. Usp.* **19** 1031 (1976); *Usp. Fiz. Nauk* **120** 705 (1976)
5. Gribov V N et al. *Phys. Lett. B* **28** 493 (1969)
6. Bilenky S et al. *Phys. Rep.* **41** 225 (1978)
7. Bilen'kii S M, Pontecorvo B *Sov. Phys. Usp.* **20** 776 (1977); *Usp. Fiz. Nauk* **123** 181 (1977)
8. Maki Z, Nakagawa M, Sakata S *Prog. Theor. Phys.* **28** 870 (1962)
9. Davis R (Jr.), Harmer D S, Hoffman K C *Phys. Rev. Lett.* **20** 1205 (1968)
10. Abdurashitov J N et al. (SAGE Collab.) *Phys. Rev. C* **60** 055801 (1999)
11. Hampel W et al. (GALLEX Collab.) *Phys. Lett. B* **447** 127 (1999)
12. Haines T et al. (IMB Collab.) *Phys. Rev. Lett.* **57** 1986 (1986)
13. Nakahata M et al. (Kamiokande Collab.) *J. Phys. Soc. Jpn.* **55** 3786 (1986)
14. Hirata K et al. (Kamiokande-II Collab.) *Phys. Lett. B* **205** 416 (1988)
15. Fukuda Y et al. (Super-Kamiokande Collab.) *Phys. Rev. Lett.* **81** 1562 (1998)
16. Smirnov A Yu, arXiv:1609.02386
17. Ahmad Q et al. (SNO Collab.) *Phys. Rev. Lett.* **89** 011301 (2002)
18. The 2016 Breakthrough prize in fundamental physics, https://breakthroughprize.org/Laureates/1/P1/Y2016
19. Eguchi K et al. (KamLAND Collab.) *Phys. Rev. Lett.* **90** 021802 (2003)
20. Abe K et al. (T2K Collab.) *Nucl. Instrum. Meth. Phys. Res. A* **659** 106 (2011)
21. Ahn M et al. (K2K Collab.) *Phys. Rev. D* **74** 072003 (2006)
22. Guo X et al. (Daya Bay Collab.), hep-ex/0701029
23. Particle Data Group, Zyla P et al. *Prog. Theor. Exp. Phys.* **2020** 083C01 (2020)
24. de Gouvêa A *Annu. Rev. Nucl. Part. Sci.* **66** 197 (2016)
25. Mohapatra R N et al. *Rep. Prog. Phys.* **70** 1757 (2007)
26. Akhmedov E Kh, in *ICTP Summer School in Particle Physics, 21 June – 9 July 1999, Trieste, Italy*, pp. 103–164; hep-ph/0001264
27. Troitsky S V *Phys. Usp.* **55** 72 (2012); *Usp. Fiz. Nauk* **182** 77 (2012)
28. Böser S et al. *Prog. Part. Nucl. Phys.* **111** 103736 (2020)
29. Gorbunov D S *Phys. Usp.* **57** 503 (2014); *Usp. Fiz. Nauk* **184** 545 (2014)
30. Dolinski M J, Poon A W P, Rodejohann W *Annu. Rev. Nucl. Part. Sci.* **69** 219 (2019)
31. Šimkovic F *Phys. Usp.* **64** 1238 (2021); *Usp. Fiz. Nauk* **191** 1307 (2021)
32. Barabash A S *Phys. Usp.* **57** 482 (2014); *Usp. Fiz. Nauk* **184** 524 (2014)
33. Aker M et al. (KATRIN Collab.), arXiv:2105.08533
34. Aartsen M G et al. (IceCube Collab.) *Phys. Rev. Lett.* **113** 101101 (2014)
35. Aartsen M G et al. *Science* **361** eaat1378 (2018)
36. Plavin A V et al. *Astrophys. J.* **908** 157 (2021)
37. Agostini M et al. (BOREXINO Collab.) *Nature* **587** 577 (2020)
38. Derbin A V *Phys. Usp.* **57** 512 (2014); *Usp. Fiz. Nauk* **184** 555 (2014)
39. Gershtein S S, Kuznetsov E P, Ryabov V A *Phys. Usp.* **40** 773 (1997); *Usp. Fiz. Nauk* **167** 811 (1997)
40. Akhmedov E Kh *Phys. Usp.* **47** 117 (2004); *Usp. Fiz. Nauk* **174** 121 (2004)
41. Bilen'kii S M *Phys. Usp.* **46** 1137 (2003); *Usp. Fiz. Nauk* **173** 1171 (2003)
42. Giunti C, Kim C W *Phys. Rev. D* **58** 017301 (1998)
43. Naumov D V, Naumov V A *J. Phys. G* **37** 105014 (2010)
44. An F P et al. (Daya Bay Collab.) *Eur. Phys. J. C* **77** 606 (2017)
45. Wolfenstein L *Phys. Rev. D* **17** 2369 (1978)
46. Mikheyev S P, Smirnov A Yu *Sov. J. Nucl. Phys.* **42** 913 (1985); *Yad. Fiz.* **42** 1441 (1985)
47. Mikheev S P, Smirnov A Yu *Sov. Phys. Usp.* **29** 1155 (1986); *Usp. Fiz. Nauk* **150** 632 (1986)
48. Mikheev S P, Smirnov A Yu *Sov. Phys. Usp.* **30** 759 (1987); *Usp. Fiz. Nauk* **153** 3 (1987)

49. Adamson P et al. (MINOS Collab.) *Phys. Rev. Lett.* **112** 191801 (2014)
50. Akhmedov E K et al. *J. High Energy Phys.* **2004** (04) 078 (2004)
51. Li Y, Wang Y, Xing Z *Chinese Phys. C* **40** 091001 (2016)
52. Khan A N, Nunokawa H, Parke S J *Phys. Lett. B* **803** 135354 (2020)
53. Sajjad Athar M et al. (IUPAP Neutrino panel) *Prog. Part. Nucl. Phys.* **124** 103947 (2022); arXiv:2111.07586
54. Kolupaeva L D, Olshevskiy A G, Samoylov O B *Phys. Part. Nuclei* **52** 357 (2021); *Fiz. Elem. Chastits Atom. Yadra* **52** 668 (2021)
55. King S F, Luhn C *Rep. Prog. Phys.* **76** 056201 (2013)
56. King S F et al. *New J. Phys.* **16** 045018 (2014)
57. Smirnov A Yu, Xu X-J *Phys. Rev. D* **97** 095030 (2018)
58. Capozzi F et al. *Phys. Rev. D* **104** 083031 (2021)
59. NuFIT v5.1, http://www.nu-fit.org
60. De Salas P F et al. *J. High Energy Phys.* **2021** (02) 071 (2021)
61. Capozzi F et al. *Phys. Rev. Lett.* **123** 131803 (2019)
62. Abe K et al. (Super-Kamiokande Collab.) *Phys. Rev. D* **94** 052010 (2016)
63. Aharmim B et al. (SNO Collab.) *Phys. Rev. C* **88** 025501 (2013)
64. https://git.jinr.ru/nu/osc
65. Nakajima Y "Recent results and future prospects from Super-Kamiokande", in *The XXIX Intern. Conf. on Neutrino Physics and Astrophysics, NEUTRINO2020, June 30, 2020*
66. Esteban I et al. *J. High Energy Phys.* **2018** (08) 180 (2018)
67. Guo X et al. (Daya Bay Collab.), hep-ex/0701029
68. Ardellier F et al. (Double CHOOZ Collab.), hep-ex/0606025
69. Ahn J et al. (RENO Collab.), arXiv:1003.1391
70. Gando A et al. (KamLAND Collab.) *Phys. Rev. D* **83** 052002 (2011)
71. Ables E et al. (MINOS Collab.), FERMILAB-PROPOSAL-0875 (1995)
72. Abe K et al. (T2K Collab.) *Phys. Rev. Lett.* **107** 041801 (2011)
73. Adamson P et al. (MINOS Collab.) *Phys. Rev. Lett.* **107** 181802 (2011)
74. Abe Y et al. (Double CHOOZ Collab.) *Phys. Rev. Lett.* **108** 131801 (2012)
75. Fogli G L et al. *Phys. Rev. D* **84** 053007 (2011)
76. An F et al. (Daya Bay Collab.) *Phys. Rev. Lett.* **108** 171803 (2012)
77. Ahn J et al. (RENO Collab) *Phys. Rev. Lett.* **108** 191802 (2012)
78. Dunne P "Latest neutrino oscillation results from T2K", in *The XXIX Intern. Conf. on Neutrino Physics and Astrophysics, NEUTRINO2020, June 30, 2020*
79. Abi B et al. (DUNE Collab.) *Eur. Phys. J. C* **80** 978 (2020)
80. An F et al. (Daya Bay Collab.) *Phys. Rev. D* **93** 072011 (2016)
81. Bezerra T "New Results from the Double Chooz Experiment", in *The XXIX Intern. Conf. on Neutrino Physics and Astrophysics, NEUTRINO2020, June 30, 2020*
82. Abusleme A et al. (JUNO Collab.) *Chinese Phys. C* **46** 123001 (2022)
83. "Scientists say farewell to Daya Bay site, proceed with final data analysis", 11 December 2020, Lawrence Berkeley National Laboratory. Interactions.org, https://www.interactions.org/press-release/scientists-say-farewell-daya-bay-site-proceed-final-data
84. Ayres D et al. (NOvA Collab.), hep-ex/0503053
85. Alekou A et al. (ESSvSB Collab.) *Eur. Phys. J. C* **81** 1130 (2021)
86. Aartsen G et al. (IceCube Collab.) *Phys. Rev. Lett.* **120** 071801 (2018)
87. Abe K et al. (Hyper-Kamiokande Proto-Collab.), arXiv:1805.04163
88. Aartsen M et al. (IceCube-Gen2 Collab.) *Phys. Rev. D* **101** 032006 (2020)
89. Ahmed S et al. (ICAL Collab.) *Pramana* **88** (5) 79 (2017)
90. Adamson P et al. (MINOS Collab.) *Phys. Rev. Lett.* **125** 131802 (2020)
91. Aiello S et al. (KM3NeT Collab.) *Eur. Phys. J. C* **82** (1) 26 (2022)
92. Ahmad S et al. (KM3NeT and JUNO Collab.), arXiv:2108.06293
93. Acero M A et al. (NOvA Collab.) *Phys. Rev. D* **106** 032004 (2022); arXiv:2108.08219
94. Abbasi R et al. (IceCube Collab.) *Astropart. Phys.* **35** 615 (2012)
95. Mohapatra R N, Nasri S, Yu H-B *Phys. Lett. B* **636** 114 (2006)
96. Mohapatra R N, Nasri C C *J. High Energy Phys.* **2015** (08) 92 (2015)
97. Minakata H, Smirnov A Yu *Phys. Rev. D* **70** 073009 (2004)
98. Babu K S, Ma E, Valle J W F *Phys. Lett. B* **552** 207 (2003)
99. Scholberg K *J. Phys. G* **45** 014002 (2018)
100. Qian X, Vogel P *Prog. Part. Nucl. Phys.* **83** 1 (2015)
101. de Salas P F et al. *Front. Astron. Space Sci.* **5** 36 (2018)
102. Pascoli S, Petcov S T, Riotto A *Phys. Rev. D* **75** 083511 (2007)
103. Branco G C, González Felipe R, Joaquim F R *Phys. Lett. B* **645** 432 (2007)
104. Davidson S et al. *Phys. Rev. Lett.* **99** 161801 (2007)
105. Branco G C et al. *Nucl. Phys. B* **617** 475 (2001)
106. Jiang M et al. (Super-Kamiokande Collab.) *Prog. Theor. Exp. Phys.* **2019** 053F01 (2019)
107. Marti Ll et al. *Nucl. Instrum. Meth. Phys. Res. A* **959** 163549 (2020)
108. Beacom J F, Vagins M R *Phys. Rev. Lett.* **93** 171101 (2004)
109. Esteban I et al. *J. High Energy Phys.* **2020** (09) 178 (2020)
110. Kudenko Yu G *Phys. Usp.* **54** 549 (2011); *Usp. Fiz. Nauk* **181** 569 (2011)
111. Kudenko Yu G *Phys. Usp.* **56** 1120 (2013); *Usp. Fiz. Nauk* **183** 1225 (2013)
112. Friend M *Nat. Rev. Phys.* **2** 2 (2020)
113. "T2k run 10 ended with record beam power". February 20, 2020. The T2K Collab., https://t2k-experiment.org/2020/02/t2k-run-10-ended-with-record-beam-power/
114. Shiltsev V, in *17th Conf. on Flavor Physics and CP Violation, FPCP 2019, 6 – 10 May 2019, Victoria, BC, Canada*; arXiv:1906.07324
115. Abe K et al. (T2K Collab.) *Nucl. Instrum. Meth. Phys. Res. A* **694** 211 (2012)
116. Assylbekov S et al. *Nucl. Instrum. Meth. Phys. Res. A* **686** 48 (2012)
117. Abgrall N et al. *Nucl. Instrum. Meth. Phys. Res. A* **637** 25 (2011)
118. Amaudruz P-A et al. *Nucl. Instrum. Meth. Phys. Res. A* **696** 1 (2012)
119. Allan D et al. *JINST* **8** P10019 (2013)
120. Aoki S et al. *Nucl. Instrum. Meth. Phys. Res. A* **698** 135 (2013)
121. Barranco-Luque M et al. (UA1 Collab.) *Nucl. Instrum. Meth.* **176** 175 (1980)
122. Antonova M et al. (Baby MIND Collab.) *JINST* **12** C07028 (2017)
123. Neutrino 2020 website, https://conferences.fnal.gov/nu2020/
124. Abe K et al. (T2K Collab.) *Nature* **580** 339 (2020)
125. Read A *J. Phys. G* **28** 2693 (2002)
126. Kelly K J et al. *Phys. Rev. D* **103** 013004 (2021)
127. Dolan S "T2K status and plans", in *EPS-HEP Conf., European Physical Society Conf. on High Energy Physics 2021, Online Conf., July 26 – 30, 2021*
128. Speagle J S, arXiv:1909.12313
129. Abe K et al. (T2K Collab.) *Phys. Rev. D* **96** 092006 (2017)
130. Bronner C "Details of T2K oscillation analysis", in *21st Intern. Workshop on Neutrinos from Accelerators, 2021*
131. Feldman G J, Cousins R D *Phys. Rev. D* **57** 3873 (1998)
132. Katori T *AIP Conf. Proc.* **1663** 030001 (2015)
133. Hayato Y *Acta Phys. Polon. B* **40** 2477 (2009)
134. Andreopoulos C et al. *Nucl. Instrum. Meth. Phys. Res. A* **614** 87 (2010)
135. Acero M A et al. (NOvA Collab.) *Eur. Phys. J. C* **80** 1119 (2020)
136. Abgrall N et al. (NA61/SHINE Collab.) *Eur. Phys. J. C* **79** 100 (2019)
137. Aliaga L et al. (MINERvA Collab.) *Phys. Rev. D* **94** 092005 (2016)
138. Barton D S et al. *Phys. Rev. D* **27** 2580 (1983)
139. Bhupal Dev P S et al. *SciPost Phys. Proc.* **2** 001 (2019)
140. Denton P B, Gehrlein J, Pestes R *Phys. Rev. Lett.* **126** 051801 (2021)
141. Chatterjee S S, Palazzo A *Phys. Rev. Lett.* **126** 051802 (2021)
142. Mitsuka G et al. (Super-Kamiokande Collab.) *Phys. Rev. D* **84** 113008 (2011)
143. Albert A et al. (ANTARES Collab.), arXiv:2112.14517
144. Ehrhardt T "Search for NSI in neutrino propagation with IceCube DeepCore", in *4th Uppsala Workshop on Particle Physics with Neutrino Telescopes, 2019*
145. Abbasi R et al. (IceCube Collab.) *Phys. Rev. Lett.* **129** 011804 (2022); arXiv:2201.03566
146. Rahaman U *Eur. Phys. J. C* **81** 792 (2021)
147. Rahaman U, Razzaque S, arXiv:2108.11783
148. Babu K S et al. *Phys. Rev. D* **105** 115014 (2022); arXiv:2108.11961
149. Chatterjee S S, Palazzo A, arXiv:2005.10338
150. Sutton A *PoS* **NuFACT2018** 058 (2018)
151. Adamson P et al. (MINOS Collab.) *Phys. Rev. Lett.* **110** 251801 (2013)
152. Abe K et al. (Super-Kamiokande Collab.) *Phys. Rev. D* **97** 072001 (2018)
153. "NOvA and T2K joint analysis announcement", https://t2k-experiment.org/2018/01/t2k-nova-announce/
154. Abe K et al. (T2K Collab.), arXiv:1901.03750
155. Blondel A et al. *JINST* **13** P02006 (2018)
156. Attié D et al. *Nucl. Instrum. Meth. Phys. Res. A* **957** 163286 (2020)
157. Korzenev A et al. *JINST* **17** P01016 (2022)
158. Abe K et al. (Hyper-Kamiokande Proto-Collab.), arXiv:1805.04163
159. Bhadra S et al. (nuPRISM Collab.), arXiv:1412.3086

160. Abi B et al. (DUNE Collab.) *JINST* **15** T08008 (2020)
161. Acciarri R et al. (DUNE Collab.), arXiv:1601.05471
162. Lebedev V, FERMILAB-DESIGN-2015-01 (2015)
163. Pellico W et al., in *5th Intern. Particle Accelerator Conf., 2014, 15 – 20 June 2014, Dresden, Germany* (Eds C Petit-Jean-Genaz et al.) (Geneva: JACoW, 2014)
164. Shiltsev V *Mod. Phys. Lett. A* **32** 1730012 (2017)
165. Prebys E et al., in *7th Intern. Particle Accelerator Conf., IPAC2016, 8 – 13 May 2016, Busan, Korea* (Eds K S Kim et al.) (Geneva: JACoW, 2016)
166. Abed Abud A et al. (DUNE Collab.) *Instruments* **5** (4) 31 (2021)
167. Anfimov N et al. *JINST* **15** C07022 (2020)
168. Agapov N N et al. *Phys. Usp.* **59** 383 (2016); *Usp. Fiz. Nauk* **186** 405 (2016)
169. Duyang H et al., arXiv:1809.08752
170. Askins M et al. (Theia Collab.) *Eur. Phys. J. C* **80** 416 (2020)
171. Yeh M et al. *Nucl. Instrum. Meth. Phys. Res. A* **660** 51 (2011)
172. Kaptanoglu T et al. *Phys. Rev. D* **101** 072002 (2020)
173. de Gouvêa A, Kelly K J *Nucl. Phys. B* **908** 318 (2016)
174. Coloma P *J. High Energy Phys.* **2016** (03) 016 (2016)
175. Bass M et al. *Phys. Rev. D* **91** 052015 (2015)
176. Abe K et al. (Hyper-Kamiokande Collab.) *Prog. Theor. Exp. Phys.* **2018** 063C01 (2018)
177. Cao J et al. (ICFA Neutrino Panel), arXiv:1501.03918
178. Guler M et al. (OPERA Collab.), CERN-SPSC-2000-028 (2000)
179. Agafonova N et al. (OPERA Collab.) *Phys. Rev. Lett.* **120** 211801 (2018)
180. Blennow M et al. *Eur. Phys. J. C* **80** 190 (2020)
181. Baussan E et al. (ESSνSB Collab.) *Nucl. Phys. B* **885** 127 (2014)
182. Bogomilov M "ESSνSB progress on the design of the near and far neutrino detectors and the simulation of the physics potential", in *XIX Intern. Workshop on Neutrino Telescopes. 2021*
183. Odagawa T (NINJA Collab.) *PoS* **NuFact2019** 144 (2020)
184. Patzak T (MEMPHYS Collab.) *J. Phys. Conf. Ser.* **375** 042055 (2012)
185. Alekou A et al. (ESSνSB Collab.) *Eur. Phys. J.C* **81** 1130 (2021)
186. Coloma P, Fernandez-Martinez E *J. High Energy Phys.* **2012** (04) 89 (2012)
187. Albright C et al., hep-ex/0008064
188. Benedikt M et al. *Eur. Phys. J. A* **47** 24 (2011)
189. Kyberd P et al. (nuStorm Collab.), arXiv:1206.0294
190. Aguilar-Arevalo A et al. (LSND Collab.) *Phys. Rev. D* **64** 112007 (2001)
191. Armbruster B et al. (KARMEN Collab.) *Phys. Rev. D* **65** 112001 (2002)
192. Aguilar-Arevalo A A et al. (MiniBooNE Collab.) *Phys. Rev. Lett.* **120** 141802 (2018)
193. Ajimura S et al. (JSNS^2 Collab.), arXiv:1705.08629
194. Rott C *PoS* **ICHEP2018** 185 (2019)
195. Alonso J R, Nakamura K (IsoDAR Collab.), arXiv:1710.09325
196. Meregaglia A *JINST* **11** C12040 (2016)
197. Denisov S *Conf. Proc. C* **880914** 207 (1988)
198. Perrin-Terrin M *Eur. Phys. J. C* **82** 465 (2022); arXiv:2112.12848
199. Kopeikin V I *Phys. Atom. Nucl.* **75** 143 (2012); *Yad. Fiz.* **75** 165 (2012)
200. Abusleme A et al. (JUNO Collab.), to be published (2021)
201. Adam T et al., arXiv:1508.07166
202. Abusleme A et al. (JUNO Collab.) *J. High Energy Phys.* **2021** (03) 004 (2021)
203. Abusleme A et al. (JUNO Collab.), arXiv:2005.08745
204. An F et al. (JUNO Collab.) *J. Phys. G* **43** 030401 (2016)
205. Abusleme A et al. (JUNO Collab.), arXiv:2104.02565
206. Abusleme A et al. (JUNO and Daya Bay Collab.) *Nucl. Instrum. Meth. Phys. Res. A* **988** 164823 (2021)
207. Huber P *Phys. Rev. C* **84** 024617 (2011)
208. Mueller T et al. *Phys. Rev. C* **83** 054615 (2011)
209. Fallot M et al. *Phys. Rev. Lett.* **109** 202504 (2012)
210. Hayes A C et al. *Annu. Rev. Nucl. Part. Sci.* **66** 219 (2016)
211. Schreckenbach K et al. *Phys. Lett. B* **160** 325 (1985)
212. Hahn A et al. *Phys. Lett. B* **218** 365 (1989)
213. Mention G et al. *Phys. Rev. D* **83** 073006 (2011)
214. Hayen L et al. *Phys. Rev. C* **100** 054323 (2019)
215. Kopeikin V I, Panin Yu N, Sabelnikov A A *Phys. Atom. Nucl.* **84** 1 (2021); *Yad. Fiz.* **84** 3 (2021)
216. Giunti C et al., arXiv:2110.06820
217. Acero M A et al., arXiv:2203.07323
218. Adey D et al. (Daya Bay Collab.) *Phys. Rev. Lett.* **123** 111801 (2019)
219. Atif Z et al. (RENO and NEOS Collab.) *Phys. Rev. D* **105** L111101 (2022)
220. de Kerret H et al. (Double CHOOZ Collab.) *Nat. Phys.* **16** 558 (2020)
221. Li Y F et al. *Phys. Rev. D* **100** 053005 (2019)
222. Dwyer D et al. *Phys. Rev. Lett.* **114** 012502 (2015)
223. Sonzogni A A et al. *Phys. Rev. C* **98** 014323 (2018)
224. An F P et al. (Daya Bay Collab.) *Chin. Phys. C* **41** 013002 (2017)
225. Abusleme A et al. (JUNO Collab.) *Eur. Phys. J. C* **81** 10 (2021)
226. Abusleme A et al. (JUNO Collab.) *Chin. Phys. C* **45** 023004 (2021)
227. Bieger L et al. *Eur. Phys. J. C* **82** 779 (2022); arXiv:2109.10782
228. Cabrera A et al. *Sci. Rep.* **12** 5393 (2022); arXiv:2008.11280
229. Aartsen M et al. (IceCube-Gen2 Collab.) *Phys. Rev. D* **101** 032006 (2020)
230. Aartsen M G et al. (IceCube Collab.) *Science* **342** 1242856 (2013)
231. Aartsen M G et al. (IceCube Collab.) *Phys. Rev. Lett.* **111** 021103 (2013)
232. Belolaptikov I, Dzhilkibaev Zh-A (on behalf of the Baikal-GVD Collab.) *PoS* **ICRC2021** 002 (2021); arXiv:2109.14344
233. Dzhilkibaev Zh-A M et al. *Phys. Usp.* **58** 495 (2015); *Usp. Fiz. Nauk* **185** 531 (2015)
234. Agostini M et al. (P-ONE Collab.) *Nat. Astron.* **4** 913 (2020)
235. Aartsen M G et al. (IceCube Collab.) *Eur. Phys. J. C* **80** (1) 9 (2020)
236. Aartsen M G et al. (IceCube Collab.) *Phys. Rev. D* **99** 032007 (2019)
237. Li Z et al. (Super-Kamiokande Collab.) *Phys. Rev. D* **98** 052006 (2018)
238. Aartsen M G et al. (IceCube-Gen2 Collab.) *J. Phys. G* **48** 060501 (2021)
239. Aartsen M G et al. (IceCube Collab.), arXiv:1911.02561
240. Haungs A (IceCube Collab.) *EPJ Web Conf.* **210** 06009 (2019)
241. Askar'yan G A *Sov. Phys. JETP* **14** 441 (1961); *Zh. Eksp. Teor. Fiz.* **41** 616 (1961)
242. Ishihara A (IceCube Collab.) *PoS* **ICRC2019** 1031 (2020)
243. Aartsen M et al. (IceCube Collab.) *J. Phys. G* **44** 054006 (2017)
244. Blot S et al., Private communication (2020)
245. Adrian-Martinez S et al. (KM3Net Collab.) *J. Phys. G* **43** 084001 (2016)
246. Ageron M et al. (ANTARES Collab.) *Nucl. Instrum. Meth. Phys. Res. A* **656** 11 (2011)
247. Aiello S et al. (KM3NeT Collab.) *Astropart. Phys.* **111** 100 (2019)
248. Akindinov A V et al. *Eur. Phys. J. C* **79** 758 (2019)
249. Hofestädt J et al. *PoS* **ICRC2019** 911 (2020)
250. Ahmed S et al. (ICAL Collab.) *Pramana* **88** (5) 79 (2017)
251. Agafonova N Y et al. (MONOLITH Collab.), LNGS-P26-2000 (2000)
252. Acero M A et al. (NOvA Collab.) *Phys. Rev. D* **106** 032004 (2022)
253. Sztuc A "A Bayesian Look at 3-flavor Oscillations in NOvA: Drilling Deeper into PMNS", Wine and Cheese seminar at FNAL (2020)
254. Abe K et al. (T2K Collab.), arXiv:2303.03222
255. de Gouvêa A et al. *Phys. Rev. D* **106** 055025 (2022)
256. Abusleme A et al. (JUNO Collab.) *Chinese Phys. C* **46** 123001 (2022)
257. Zhao J "JUNO Status and Prospects", in *NEUTRINO-2022 Conf., 2022*
258. Alekou A et al. (ESSνSB Collab.), arXiv:2303.17356
259. Neutrino 2022 website, https://neutrino2022.org
260. Stuttard T "Particle physics with atmospheric neutrinos at IceCube", in *NEUTRINO-2022 Conf., 2022*
261. Wan L "New Results with Atmospheric Neutrinos at Super-Kamiokande", in *NEUTRINO-2022 Conf., 2022*
262. Kwang K "Results of reactor antineutrinos at RENO", in *NEUTRINO-2022 Conf., 2022*
263. Cabrera A "The SuperChooz Experiment: Unveiling the Opportunity", Seminar at CERN (Geneva: CERN, 2022)
264. An F et al. (Daya Bay Collab.), arXiv:2211.14988
265. An F et al. (Daya Bay Collab.) *Phys. Rev. Lett.* **129** 041801 (2022)
266. Nguyen H C et al. *Phys. Rev. D* **108** 023013 (2023); arXiv:2212.14170
267. Spiering Ch *Phys. Usp.* **64** 1198 (2021); *Usp. Fiz. Nauk* **191** 1261 (2021)
268. Troitsky S V *Phys. Usp.* **64** 1261 (2021); *Usp. Fiz. Nauk* **191** 1333 (2021)